Modelling the impact of anthropogenic measures on saltwater intrusion in the Weser estuary

Pia Kolb[1], Anna Zorndt[1], Hans Burchard[2], Ulf Gräwe[2], and Frank Kösters[1]

[1]Federal Waterways Engineering and Research Institute, Wedeler Landstraße 157, 22559 Hamburg, Germany
[2]Leibniz Institute for Baltic Sea Research Warnemünde, Seestraße 15, 18119 Rostock, Germany

Correspondence to: Pia Kolb (pia.kolb@baw.de)

Reply to referee #1

Dear referee #1,

thank you for taking the time to read our manuscript, and for your detailed and valuable feedback. We highly appreciate your inputs, which helped us to hopefully substantially improve our paper. Please find below our responses to your comments (in italics).

General comments

The manuscript presents results from a modelling study of how changes in bathymetry of the Weser estuary affect the salinity intrusion. The study evaluates four time periods and calibrates them separately to account for variability in data availability. The main result is that dredging has resulted in a modest increase in the salinity intrusion, but this is only apparent using comparable forcing conditions because the mean change in salinity intrusion is much less than the natural variability with river discharge.

Overall the manuscript is well written and contains appropriate citations. Separately calibrating the different time periods is a distinctive approach which makes sense if there are data available to support the model evaluation, but that may not always be the case. The results presented here are broadly consistent with similar studies, and it could be a valuable contribution to the literature on the topic of anthropogenic modification of estuaries. However, I have a couple of general comments on how the analysis could be clarified to examine the physical processes more substantively and make the results more broadly applicable.

- The approach of calibrating to multiple time periods results in different optimal friction parameters among the different periods. This is attributed to differences in along-estuary depth variability (Table 1), which is explained by differences in bathymetric data resolution. The differences among most of the years are quite modest (5-20%), and are much smaller than the "additional roughness" imposed to represent tidal damping (line 258) or the variation in the effective roughness (Table 3). Additional analysis explaining this conclusion would be helpful. In particular, it's not clear how the variation in bathymetric data density (e.g., soundings from hydrographic surveys?) compares with the model grid resolution. The grid resolution is 50-250 m, and so the bathymetric data resolution would have to be lower than this to influence model results. It's also not clear whether the difference in effective roughness may instead be due to differences in sub-grid scale roughness, which is not represented directly in the grid regardless of the bathymetric survey density. The model uses a roughness parameter based on sediment characteristics (grain size), and this does not change among the years. There are certainly examples from other modified estuaries where changes in bed sediment characteristics directly affect the friction, and that would be a different mechanism than is suggested here. For example, fine sediment accumulation in the Ems reduced friction and amplified the tides (Winterwerp et al 2013), or removal of sand waves by dredging in the Columbia reduced friction and amplified the tides (Jay et al. 2011). Perhaps it is impossible to isolate the reason for the differences in calibration values among the periods, but a more thorough explanation of the proposed mechanism and assessment of alternative explanations would build confidence in the results. See below for related comments.

Reply*: In order to answer your question, we have to briefly go into details of the hydronumerical model. When constructing the numerical grid for the UnTRIM model a so-called volume preservation is used which ensures that the water volume in the model agrees exactly with the average depths of the bathymetric data. Therefore, even subgrid information enters the model when the volume is concerned. This is different for roughness. In nature, roughness can be seen as the sum of grain and form related roughness. Grain related roughness is almost negligibly small and can be neglected for the discussion here. Form roughness which in turn can be seen as the sum of the effects of ripples, mega-ripples and dunes is represented in the model in different ways. Ripples and mega-ripples are modelled based on a roughness predictor taking into account grain sizes and flow regime. The effect of dunes could not be reliably modelled based on the predictor but had to be prescribed as additional roughness. The amount of additional roughness in turn is depending on grid resolution and bathymetric data. Dunes are to some extent depicted by the numerical grid – if present in the bathymetric data. In the examined years prior to 2012 bathymetric data almost did not resolve dunes. However, even for the year 2012 with dunes represented in the bathymetric data, the numerical model represents dunes only to a limited amount as the model resolution is coarse compared to the wavelength of the dunes.*

We agree that the differences in depth resolution between 1966, 1972, and 1981 are small and might not explain the differences in the roughness settings between these models, which are determined in the calibration. We think that particularly the differences in depth resolution in the Lower Weser between 2012 and the other models can have a clear effect and need compensation. However, we decided to omit the analysis of the depth variation, because it seems to be rather confusing than helpful and can be easily misinterpreted. Instead, we now illustrate how bathymetrical data with different resolutions are represented in the models with images of different model topographies.

Action*: We edited the text in Sections 3.2 and 3.6 and hopefully, it is clearer now. We omitted the analysis of the depth variation (former Table 1) and instead added images of sections from two different model topographies (see Fig. 2b and c), which we describe in Section 3.2.*

- Part of the analysis examines differences (which are small) in the exponential regression between salinity intrusion and river discharge. This has been done in previous studies, and presumably is meant to be linked with analytical expressions for salinity vs discharge based on different assumptions about the dominant salt flux mechanisms. For example, salt flux dominated by the estuarine exchange scales with Q^(-1/3), whereas tidally dominated salt flux scales as Q^-1. Explanation of this in the text would help readers understand the motivation for examining the regressions. However, the idealized analytical frameworks don't necessarily apply to real estuaries with spatially variable bathymetry, and instead estuary shape can have a dominant influence on observed relationships with discharge. This makes it hard to link temporal variation in the exponent for Q to changes in salt flux mechanisms. Instead, it would be better to calculate salt fluxes directly in the model and quantify changes (if any) in the decomposed components (estuarine exchange vs tidal correlations). This could be particularly interesting for this system, as there is the suggestion that tidal processes are important for salt flux because the results mention that the salinity intrusion is greater during spring tides than neap tides. It likely also would require examination of the changes in tidal amplitude over time to aid in interpretation of the salinity dynamics. A previous study of the Hudson is referenced on changes in salt flux processes with dredging, but the Hudson is dominated by the estuarine exchange and not tidal salt flux. Deepening and reduction in friction with dredging generally increase tidal amplitude, which would tend to _decrease_ the estuarine exchange flow but _increase_ the tidal salt flux. The Weser could be an interesting and contrasting example to the previous studies as how the salinity intrusion responds to dredging in a tidally dominated system. It would be nice to see this aspect of the results explored in greater detail.

***Reply**: Thank you for pointing out the missing link between our regression analysis and analytical models, which we included in the manuscript now. We did so after considering the alternative, to omit this analysis completely. We think that this straightforward analysis allows to grasp easily the changes in saltwater intrusion taking into account variable river discharge. Following your suggestion, we also included a more complete analysis of the salt flux components for a representative cross-section. Our results confirm that the Weser is dominated by tidal salt flux, not by estuarine exchange (see Section 4.6.1).*

***Action**: We included the analysis of salt flux components in our paper (see Section 3.5.2 and 4.6.1) and applied the implications thereof to the other chapters, shifting the focus towards an analysis of all processes. With means of this method, further interesting questions arise that could be examined in additional analyses. As we feel this is beyond the scope of the paper, we included some of these ideas in the discussion section. We also added the important aspect that the Hudsen is dominated by estuarine circulation, in contrast to Weser estuary, in the discussion of our results (Section 5).*

Specific comments

Additional, specific comments follow with line numbers.

[25] Perhaps “masked” rather than “outweighed” (unless there was a shift in the mean discharge that was compensating for the shift in the mean depth).

***Action**: We changed “outweighed” to “masked”.*

[48] “other drivers” of what?

***Action**: We changed it: "Salt transport is also controlled by"*

[76] “Ems has successively become finer…” In the other cases (Hudson, Seine, Danshui), were changes in bed composition coincident with the changes in depth? If not, is there still need to recalibrate, presuming similar numerical grid resolution and bathymetric data (sounding density, which is the often case in systems with a long history of navigational use)? Could this include changes in bedforms with dredging (removal of sand waves)?

***Reply**: Even presuming an ideal data coverage and data quality, there would still be a need to recalibrate as roughness predictors are unfortunately still not perfect. They could hopefully significantly reduce the amount of calibration required, if changes in bed composition can be reliably determined. Changes in bedforms, such as a removal of sand waves, will probably not be feasible at subgrid level in the foreseeable future, roughness predictors usually assume an undisturbed system. Possibly these effects can be considered in roughness predictors but even then, some amount of calibration will be necessary.*

***Action**: We included a discussion in which case individual calibration might be needed and in which case not (see Section 5). Furthermore, we describe in more detail how bathymetrical data and bed forms are represented in the model topographies (see Section 3.2 and 3.6).*

[78] The bathymetric data resolution has to be considered in conjunction with the bathymetry data and the model grid resolution. Is the assumption here that the grid resolution exceeds the bathymetry data resolution? Is that often the case? It seems like it would not be the case in most estuaries with data collected for navigational charts.

***Reply**: In our case, the data resolution for historical topographies was similar or lower than the grid resolution especially in the area of Lower Weser. This might also be the case for other estuaries with respect to historical topographical data.*

***Action**: We added information about the type and resolution of topographical data in Section 3.2. We further changed "with an effect on form drag" to "which can have an effect on form drag", to indicate that there is not necessarily an effect – it depends on the respective resolutions.*

[80] "different calibrations…" Does this presume similar availability of observations (water level, salinity) for calibration? Is there a tradeoff where diminished availability of historical data to use in the calibration would degrade the confidence in the historical calibration to the point that it would be better to use the more robust and data-constrained modern calibration?

***Reply**: Of course, there are cases when an individual calibration does not make sense.*

***Action**: We adjusted the text and included the aspect in our discussion (Section 5): "It has to be noted that calibration is only possible if observational data are available to support a robust calibration. Recalibration with imprecise data of low resolution might even negatively affect model results. In addition, it might not always be necessary, depending on the representation of roughness and sediments, and the resolutions of bathymetric data and grid."*

[89] "impact is larger…" impact of what?

***Reply**: This refers to the non-linear relationship between discharge and saltwater intrusion – for example, an increase from 100 to 200 m³/s would induce a stronger shift of the salinity front compared to an increase from 800 to 900 m³/s.*

***Action**: We changed the sentence to make it clearer: "... whereby the impact of discharge variations is larger for low-discharge than high-discharge conditions."*

[92] Are “anthropogenic measures” just dredging or does it include other modifications (shoreline reclamation/hardening, discharge regulation, etc)?

***Reply**: Between all examined scenarios, deepening measures have been conducted. In addition to that, there were some other comparatively small interventions which we describe in Section 2.2. We examine the overall effect of variations in topography (which also includes natural variations), as represented in the different topographies. Based on that, we derive conclusions on the effect of deepening measures, which most strongly contribute to the topographical variations between the scenarios.*

***Action**: We added "in particular deepening measures".*

[123] “between Brake and Bremen…” Note distances from the mouth for context and to help with the interpretation of Fig 2.

***Action**: We included it in the manuscript.*

[143] What are the values of the horizontal viscosity and diffusivity?

***Reply**: The model is set-up with constant viscosity (0.1 $m^2 s^{-1}$) and diffusivity (0.1 $m^2 s^{-1}$) for all experiments.*

***Action**: We included the information in the manuscript.*

[164] “data were scarcer…” Can this be quantified by comparing the bathymetric sounding data density (if that's what was used) to the grid resolution for the different eras? It could be a range if spatially variable, but would be helpful for context particularly given the importance placed on the data density.

***Action**: We included more detailed information on the type and resolution of the bathymetric data which were used in Section 3.2.*

[165] “the resolution of small-scale features such as bedforms in the different model topographies is not directly comparable”. It seems like most bedforms aren't represented in the model grid with resolution of 50-250 m. For example, sand waves that are 1 m high and a steepness of 0.05 have a wavelength of 20 m. Perhaps clarify what is meant by "small-scale" and what types/sizes of bedforms?

***Reply**: Maybe the term "small-scale" was misleading.*

***Action**: We omitted the term "small-scale" and added detailed information on how bed forms are represented in the model topographies (see Section 3.6).*

[177] “Minor differences in depth variation do also occur between the individual model topographies” What does this mean?

***Reply**: We wanted to say that there are small differences in depth resolution between all model topographies, i.e. 1966, 1972, 1981, 2012 (see Table 1). Not only between historical topographies vs. 2012.*

***Action**: We decided to omit the analysis of the depth resolution, because it seemed not to be helpful (see above).*

[178] “the different resolutions of the underlying bathymetric data.” As noted above, it'd be useful to quantify this directly and report it relative to the model grid resolution.

***Action**: We added the information in the second paragraph of 3.2.*

[Table 1] The listed differences in roughness do not seem large – it seems like other than 2012 in the seaward section the values are essentially the same. Are the differences in roughness significant compared to the other sources of uncertainty in the data and model? This could be tested by smoothing the bathymetry to be comparable to previous years and seeing how the calibration changes.

***Action**: Within the reviewing period, we did not have time for additional simulations, but we included the idea in our discussion. With regard to the depth variation, we decided to omit it (see above).*

[191] It seems like changes in the sediment composition could be a bigger effect than the small changes in the variance at the grid scale listed in Table 1. If dredging is removing sand waves or leading to finer bed sediment with increased deposition, then this would reduce the bottom roughness. Perhaps that has the same effect as is being implied by the changes in grid-scale roughness? The grid scale roughness of ~0.15-0.3m variability over 50 m (Table 1) gives a bedform steepness of 0.003-0.006, which is much less steep than the sand waves and other bedforms that would be subgrid scale and could dominate the roughness represented by z0.

***Reply**: We agree that the effect of changes in sediments and bedforms on calibration results can be equally important compared to the effect of different resolutions of topographical data.*

***Action**: We deleted the sentence: "We assume that the effect of this simplification is small." We rewrote Section 3.6 to make it clearer and added information how bed forms are represented in the model topographies.*

[212] Did you quantify the "error" in the neural network salinity by comparing the model results to the observations? That could provide some context for interpreting the uncertainty in the periods without observations at the boundary.

***Action**: We added the information in the manuscript.*

[245] “An increase in potential energy anomaly indicates an increase in stratification…” Clarify that this assumes a constant water level \eta.

***Action**: We added it in the manuscript.*

[257] Is the additional roughness spatially varying? Is it related to a physical parameter (e.g., mean depth, grain size, or distance along the channel, etc) or is it allowed to vary independently?

***Reply**: The additional roughness is spatially varying, it was defined during calibration to best possibly represent the damping of the tidal wave along the estuary. It is not related to a physical parameter.*

***Action**: We added more information in the text: "The additional roughness increases from Weser-km 55 towards Weser-km 26 and decreases afterwards again. In this way, damping of the tidal wave could be well represented."*

[260] Are the dunes and ripples not represented in the model grid because the van Rijn formulation does not match up with observed ripple size/steepness? Or is it that the grain size in the model does not match that in the real world? Please clarify.

***Action**: We now describe this aspect in Section 3.6.*

[270] Omission of tributaries is mentioned as a reason for additional roughness, but is the presence/absence of tributaries different among the cases? If so, it seems that would not explain differences in the calibration among the periods?

***Reply**: Mainly, we think that the omission of tributaries can explain why an additional roughness had to be defined in the Lower Weser for all scenarios. In combination with other factors (for example inaccuracies in topographical data), it could also strengthen model inaccuracies in individual models.*

***Action**: We rewrote parts of Section 3.6 and hopefully it is clearer now.*

[295] The result that the salinity intrusion is farther landward during spring tides seems notable, in that in many other systems where salinity has shifted with deepening the gravitational circulation dominates the landward salt flux, so salinity intrusion is maximum during neap tides. Perhaps this will be addressed in the discussion.

***Action**: We included the aspect in our discussion.*

[342] The difference in exponent may be statistically significant (i.e., unlikely to be due to chance), but it is still really small (0.164 vs 0.145), so it perhaps it’s not so important? Any difference in salt flux mechanisms associated with that small a change would be subtle, and it'd be hard to ascribe the differences in transport processes to the exponents alone. If that topic were of interest, diagnosing the salt flux mechanisms in the model directly would be the way to do it.

***Reply**: We agree that it was unclear in the text whether the difference in exponents can link to differences in processes or not.*

***Action**: We adjusted the text to clarify that, in our view, the difference is too small to allow for such conclusions. Instead, we analyzed salt flux mechanisms in Section 4.6.1.*

[342] This p-value should be reported as (p< .001) since it is not exactly 0 but rather 0.000 to three decimal places.

***Action**: We changed it in the manuscript.*

[387] "saltwater intrusion length is similar in the four scenarios." While the differences in salinity intrusion are smaller than in the case with different roughnesses, the trends are similar (1972 and 1966 similar and shorter than 2021 and 1981), and it seems inaccurate to say the four scenarios are similar.

***Reply**: The four scenarios are not similar, but the trend is not as clear compared to the simulations with recalibrated models.*

***Action**: We changed it in the manuscript.*

[390] "less energy dissipation…" It would be valuable to diagnose this directly with analysis of the differences in tidal amplitude. Presumably, the roughness affects the tides, which then affects the salt transport. Showing the "why" of this response would clarify the physics and make it more transferable to other systems.

***Action**: We added in the manuscript: "simulations with identical roughness settings do not adequately reproduce tidal energy, e.g. the tidal range in 1981 is larger than in 2012 contrary to observations. The erroneously increased tidal range exceeds the effect of changes in other processes, so that the limit of saltwater intrusion shifts seawards, and not landwards, between 1981 and 2012."*

[414] "As expected…" Is it expected because of the river discharge? It'd be worth stating directly.

***Action**: We added it in the manuscript.*

[417] "Through the increase of the landward relative to seaward volume transport and river discharge, saltwater intrudes further into the estuary." It's not obvious that this must be the case. If the volume transport scales with the tidal velocity and the difference between landward and seaward volume transport scales with the river discharge, then increasing the tidal velocities can have the opposite effect of reducing the estuarine circulation and mean stratification, thereby reducing the salinity intrusion. The salt transport in the Weser may be predominantly due to tidal processes rather than the mean circulation, but this should be explained, and the changes shown.

***Reply**: Thank you for pointing out the ambiguity in our interpretation. Based on the analysis of the salt fluxes (Section 4.6.1) we can now confirm that transport in Weser estuary is predominantly dominated by tidal processes.*

[443] “Therefore, the small difference between 1966 and 1981 cannot be clearly attributed to a change in salt flux mechanisms.” This is repetitive of a previous section, and if the question is about changes in salt flux mechanisms then that should be analyzed in the model results directly.

***Action**: We combined the paragraph with Section 4.3 to avoid repetition and make the paper more concise.*

[460] “However, models representing historical system states are often not calibrated” In the citations here, Ralston and Geyer compares their model with historical salinity data (Fig 6 and Fig 7), and Grasso and Le Hir and Liu et al. calculate model skills for their modern model configurations. Perhaps this should be recast to say that recalibration is only necessary 1) if the model grid does not capture changes in roughness that affect model skill, and 2) there are observational data to support a robust calibration?

***Action**: We agree and included the aspects in our discussion.*

[463] “We recommend…” Related to the previous comment, it is usually a lack of observational data that limits historical model calibration. What's the recommendation in that case? How do the "artificial surface irregularities" suggested to compensate for low resolution data relate to changes in topography at larger scales by dredging? One could imagine the irregularities being bigger (deeper channel=bigger sand waves) or smaller (maintenance dredging planes off big sand waves).

***Action**: In our discussion, we included some ideas when calibration might be needed and when not. The sentence about artificial surface irregularities is now in Section 3.6, we combined some sections to make the text more concise and avoid repetition. To clarify, we changed the sentence: “Alternatively, the low resolution of historical bathymetric data could be compensated by adding artificial surface irregularities, which represent the depth variation due to e.g. sand waves, as implemented by Hubert et al. (2021).“*

[486] What are the “analytical descriptions”? Is the suggestion that the variance from the power-law is greater for the Weser than for other systems? Or does it refer to the difference between -0.28 and -0.15 for the Hudson vs the Weser? That could reflect differences in transport processes and bathymetry between the systems, but does not necessarily mean that either is more or less "limited" in using this approach to characterize the relationship between discharge and salinity.

***Action**: We changed it in the manuscript: “The large difference from the sensitivity found in our study could be related to differences in bathymetry and transport processes between the estuaries. While saltwater intrusion into the Hudson is dominated by estuarine exchange flow, we show that the Weser is dominated by tidal pumping (see Section 4.6.1).”*

References

Hubert, K., Wurpts, A., & Berkenbrink, C. (2021). Interaction of Estuarine Morphology and adjacent Coastal Water Tidal Dynamics (ALADYN-C). Die Küste, 89, 193–217. https://doi.org/10.18171/1.089108

Jay, D. A., Leffler, K., & Degens, S. (2011). Long-term evolution of Columbia River tides. Journal of Waterway, Port, Coastal, and Ocean Engineering, 137(4), 182–191. https://doi.org/10.1061/(ASCE)WW.1943-5460.0000082

Winterwerp, J. C., Wang, Z. B., van Braeckel, A., van Holland, G., & Kösters, F. (2013). Man-induced regime shifts in small estuaries—II: A comparison of rivers. Ocean Dynamics, 63(11–12), 1293–1306. https://doi.org/10.1007/s10236-013-0663-8

Reply to referee #2

Dear referee #2,

thank you for taking the time to read our manuscript, and for your detailed and helpful feedback. We highly appreciate your inputs and hope that all ambiguities are resolved now. Please find below our responses to your comments (in italics).

General comments

The authors conducted a series of numerical experiments to investigate impact of historic engineering on salt intrusion in the Weser estuary. Their methods are valid, figures and tables are clear, some findings are interesting and useful.

My major concern about their paper is that the authors assume estuarine circulation (or vertical exchange flow) is the only landward salt transport process about the salt transport processes. In addition to vertical shear dispersion, tidal pumping can act as an important salt transport mechanism in well mixed estuaries (Wei et al., 2016), weakly stratified estuaries (Wei et al 2021) and partially mixed estuaries (Uncles et al 1985). Uncles et al. (1985) also pointed out importance of transverse shear dispersion in wide sections. The Weser estuary is relatively long (>120 km) with a tidal range of 2.8-4.1 m, it is very likely that tidal pumping plays a significant role in salt transport here. Lateral shear dispersion may be also important in the wide Outer Weser.

These additional processes might help to explain the difference in the relationship between salt intrusion length and river discharge in the Weser with that in the Hudson estuary found by Ralston and Geyer (2019), where the vertical shear dispersion due to gravitational circulation was assumed to dominate the landward salt transport. I suggest the authors systematically explore the dominant processes of salt transport in all experiments and attribute changes in responses of salt intrusion (if any) to those processes. This should also help increase the impact of their study, for example, by making their findings applicable to other estuaries dominated by similar processes.

***Reply**: Thank you for pointing out the different mechanisms of salt transport. A general overview of these processes is given in our Introduction but their detailed analysis was not so much in the focus of our paper. Following your recommendation and that of reviewer #1 we conducted a decomposition of the salt flux components based on a method described by Becherer et al. (2016). We can confirm now the significant role of tidal pumping which was previously not explicitly described in our paper.*

***Action**: We described results of the salt flux decomposition in Section 4.6.1. In light of this additional analysis, we re-evaluated our results from the analysis of salt intrusion length vs. river discharge.*

Specific comments

Other comments:

Figure 1: can you show the bathymetry map of the Weser with topography data of 2012?

***Action**: We included the topographical data in the map.*

Line 140: how large are the horizontal mixing coefficients? Is it the same constant for all experiments?

***Reply**: The model is set-up with constant viscosity (0.1 $m^2 s^{-1}$) and diffusivity (0.1 $m^2 s^{-1}$) for all experiments.*

***Action**: We added the information in the manuscript.*

Line 140-145. "UnTRIM² was coupled with the sediment transport model SediMorph (BAW, 2002) to calculate bottom roughness. For simplicity, we neglected sediment transport in this study". These two sentences seem contradictory.

***Reply**: The model SediMorph was used for the calculation of bottom roughness (based on prescribed sediment data), but not for the calculation of the transport of sediments.*

***Action**: We changed the phrasing: "UnTRIM² was coupled with the sediment transport model SediMorph (BAW, 2002), but only to calculate bottom roughness. Sediment transport was neglected in this study."*

Line 165: "the resolution of small-scale features such as bedforms in the different model topographies is not directly comparable." Can you show the bathymetry maps of different years as supplementary figures?

***Reply**: In order to illustrate the resolution of small-scale features we included sections of model topography 1972 and model topography 2012 in the manuscript (Fig. 2b and c). Maps covering a larger area would not allow to distinguish details of the resolution. Instead, we refer to the historical digital terrain model data, which we have added as an asset (linked to our paper on the EGUsphere website) and cited in our manuscript. The historical digital terrain model data can be found at https://doi.org/10.48437/02.2020.K2.5200.0001.*

***Action**: To better demonstrate the effect of the different resolution of topographical data of different years, we included sections of model topography 1972 and model topography 2012 in the manuscript (Fig. 2b and c).*

Line 255, "…with some variations among models." How different are the increased roughness in the lower Weser (landward side of Weser-km 55) across all experiments? How sensitive are salinity results to this increased roughness?

***Reply**: The additional roughness in the Lower Weser is spatially varying. It ranges from up to 0.22 m (system state 2012) to up to 0.36 m (system state 1981).*

***Action**: We added: "The additional roughness increases from Weser-km 55 towards Weser-km 26 and decreases afterwards again […] the maximum additional roughness ranges from 0.22 m (system state 2012) to 0.36 m (system state 1981)". We also edited Table 3 to now show the average bed roughness along the navigation channel for all models.*

Line 250-260. Can you show the estimated form roughness for each experiment? How large is the simulated form roughness compared to the additionally increased roughness?

***Reply**: While the estimated form roughness is in the range of 0.01 to 0.04 m, the maximum additional roughness ranges from 0.22 m (system state 2012) to 0.36 m (system state 1981).*

Action*: We added the information in the text in Section 3.6.*

Figure 3: Model calibration with tidal range only, how about the tidal phase and tidal/residual currents? If exchange flow is the dominant salt transport process, it is essential to make sure the model reproduces the residual currents well. Right?

Reply*: For each model, different roughness settings were determined by comparing model results with water level time series, if available (system state 2012), and the tidal range (all scenarios). Furthermore, a visual inspection of observed and modelled water levels was conducted concerning the phasing of tides. We agree that calibration with regard to residual tidal currents could have helped to further validate or improve our models. However, we think that a robust analysis concerning residual currents is difficult based on the data quality of tidal currents available.*

Action*: In our validation, we added: "The mean RMSE for the comparison of modelled and observed water levels in 2012 was 0.22 m, averaged over all measurement stations (see Figure 1) […] A visual inspection of observed and modelled water levels suggested a correct phasing of tides, which is corroborated by the low RMSE."*

Line 285: intertidal --> intratidal

Action*: We changed it in the text.*

Line 294-295. The fact that salt intrusion increases with increasing tidal range also suggests tidal pumping as an important landward salt transport agent.

Reply*: Yes. Results indicate that salt flux in the Weser estuary is dominated by tidal pumping contributions and advective flux. This also explains the result that saltwater intrusion is farther landward during spring tides compared to neap tides*

Action*: We analyze salt flux processes in Section 4.6.1 and discuss implications for the spring-neap variability in Section 5.*

Figure 4. the ticks of the x-axis are not aligned with the labels.

Action*: We corrected it.*

Line 309: tide level --> tidal level

Action*: We changed it in the text.*

Line 319-321: salt intrusion length has already been defined on line 238-239.

Action*: We deleted the repeated definition.*

Line 322-335: this part is more suitable for the Methods section.

***Action**: We agree, we shifted it to the methods section.*

Line 344-345: did salt transport mechanisms change from 1966 to 1981?

***Reply**: We think that the change in exponents is too small to support this interpretation.*

***Action**: To make the text clearer, we deleted „pointing to a change in the system between 1966 and 1981".*

Line 353: "2012 – however, …" --> 2012. However, …

***Action**: We changed it in the text.*

Line 373-374: Delete the content in the bracket as you have already defined brackish water zone.

***Action**: We deleted it.*

Line 381: this sentence is misleading. You didn"t include sediment transport or morphological evolution in the model, right?

***Reply**: We wanted to express that changes in roughness occur over time in the actual estuary, so roughness would be different for the scenarios which we represent with our models. This (along with other effects) would be visible in the calibration, when different roughness settings are determined for different scenarios.*

***Action**: We edited the paragraph – hopefully, it is clear now.*

Line 400: estuarine circulation is not the only important salt transport process for every estuary. See my major comment above.

***Reply**: Yes. See our comments and actions above.*

Line 440-444: what about responses of salt intrusion length to tides? Did it change?

***Reply**: Topography changes can influence tides in the estuary, e. g. the tidal range may increase due to increasing depths. For the Weser estuary, this effect is confirmed in the simulations with identical forcing. Taking the tidal range at Weser-km 60 as an example it increases from 3.65 m in 1966, 3.67 m in 1972, 3.86 m in 1981, to 3.88 m in 2012.*

***Action**: We included this aspect in Section 4.6.*

The paper is lengthy with quite some information repeated. I suggest the authors to remove repetitive and unnecessary contents to make the paper more concise.

***Reply**: Thank you for your advice. Due to the additional explanations and the additional analysis added in the reviewing process, the paper did not become overall shorter in the end. We hope it is nevertheless more concise now.*

***Action**: We removed repetitive sections (e.g. previous Section 4.6.3) and combined paragraphs to make the text more concise. In particular, we noticed that aspects related to roughness and calibration were discussed in several sections, which had caused repetitions. We now discuss reasons for the different roughness settings determined by calibration solely in Section 3.6. In Section 5, we discuss in which case individual calibration of each model is required and in which case it may not be required. To make the text shorter, we further deleted some unnecessary content, such as the analysis of the bottom and surface current velocity and the analysis of the depth variation.*

References:

BAW (2002). Mathematical Module Sedimorph: Validation Document Version 1.1.

Becherer, J., Flöser, G., Umlauf, L., and Burchard, H (2016). Estuarine circulation versus tidal pumping: Sediment transport in a well-mixed tidal inlet, J. Geophys. Res. Oceans, 121, 6251–6270, https://doi.org/10.1002/2016JC011640.

Uncles, R. J., Elliott, R. C. A., & Weston, S. A. (1985). Dispersion of salt and suspended sediment in a partly mixed estuary. Estuaries, 8(3), 256-269.

Wei, X., Schramkowski, G. P., & Schuttelaars, H. M. (2016). Salt dynamics in well-mixed estuaries: Importance of advection by tides. Journal of Physical Oceanography, 46(5), 1457-1475.

Wei, X., Schuttelaars, H. M., Williams, M. E., Brown, J. M., Thorne, P. D., & Amoudry, L. O. (2021). Unraveling interactions between asymmetric tidal turbulence, residual circulation, and salinity dynamics in short, periodically weakly stratified estuaries. Journal of Physical Oceanography, 51(5), 1395-1416.

Modelling the impact of anthropogenic measures on saltwater intrusion in the Weser estuary

Pia Kolb[1], Anna Zorndt[1], Hans Burchard[2], Ulf Gräwe[2], and Frank Kösters[1]

[1]Federal Waterways Engineering and Research Institute, Wedeler Landstraße 157, 22559 Hamburg, Germany
[2]Leibniz Institute for Baltic Sea Research Warnemünde, Seestraße 15, 18119 Rostock, Germany

Correspondence to: Pia Kolb (pia.kolb@baw.de)

Abstract. The Weser estuary has been subject to profound changes in topography in the last hundred years through natural variations and river engineering measures, leading to strong changes in hydrodynamics. These changes are also expected to have affected the dynamics of saltwater intrusion. Using numerical modelling, we examined saltwater intrusion in the Weser estuary in four different system states (1966, 1972, 1981, 2012). Models of each system state were set up with the respective topography and boundary values. ~~The~~We calibrated and validated each model individually to account for differences in sediments, bedforms, and the resolution of underlying bathymetric data between historical and recent ~~topographical data is usually not comparable, which needs to be compensated, e.g., by calibration of roughness parameters. Therefore, each model was individually calibrated and validated.~~system states. In simulations of one hydrological year ~~for~~ each ~~system state~~with realistic forcing (hindcasting study), the influence of topography is overshadowed by the effects of other factors, particularly river discharge. At times of identical discharge, results indicate a landward shift of the salinity front between 1966 and 2012. Subsequent simulations with different topographies but identical boundary conditions (scenario study) confirm that ~~topographic~~topography changes in the Weser estuary affected saltwater intrusion. Solely through the topography changes, at a discharge of 300 m³ s^{-1}, the position of the tidally averaged and depth-averaged salinity front shifted landwards by about 2.5 km between 1972 and 1981 ~~due to deepening measures in the Lower Weser between these years. It shifted~~and by another 1 km between 1981 and 2012. These changes are significant but comparatively small, since due to seasonal variations in run-off, the tidally averaged ~~salinity intrusion can vary by more than 20 km.~~saltwater intrusion can vary by more than 20 km. Moreover, our analysis has shown that saltwater intrusion in the Weser estuary is primarily driven by tidal pumping and only to a lesser degree due to estuarine circulation. The shift between 1972 and 1981 is likely caused by an increase in estuarine circulation in response to deepening measures in the Lower Weser.

Short summary:

River engineering measures strongly changed tidal dynamics in the Weser estuary. We studied the effect on saltwater intrusion with numerical models. Our analysis shows that a deepening of the navigation channel causes saltwater to intrude further into the Weser estuary. This effect is mostly ~~outweighed~~masked by the natural variability of river discharge. In ~~the~~our study, it proved essential to recalibrate individual hindcast models due to ~~different resolutions of~~differences in sediments, bed forms, and underlying ~~bathymetrical~~bathymetric data.

Keywords: Estuaries, numerical models, shelf seas, seabed morphology, Weser estuary, estuary deepening, morphological changes, saltwater intrusion

1 Introduction

Estuaries are ever-changing systems. Natural processes and anthropogenic interventions determine the topography and conditions we observe in estuaries today. Due to the high economic importance of estuaries as shipping routes, further interventions to consolidate navigation channels can be expected. In order to manage adverse effects, predictability of changes associated with the engineering measures is essential. As a response to deepening measures, significant changes in hydrodynamics have been observed in estuaries. When water depth increases, the effect of bottom friction decreases. This reduces the dissipation of tidal energy, resulting in a larger tidal amplitude and often in phase shifts in the ebb and flood current durations and velocities (Winterwerp et al., 2013; Ralston et al., 2019). At the same time, changes in mixing processes can occur, possibly affecting the length of saltwater intrusion (Grasso and Le Hir, 2019). Saltwater intrusion is directly linked to water quality and sediment transport processes (Burchard et al., 2018a) and thus needs to be monitored.

The effect of topography changes on saltwater intrusion depends on the physical mechanisms that control salt transport in estuaries. Most important are the net advection, driven by freshwater discharge, tidal asymmetry effects, and the estuarine circulation, i.e. the tidally averaged estuarine exchange flow. One driver of the estuarine circulation is the combination of the seaward barotropic (depth-independent) and the landward baroclinic (increasing with depth) pressure gradient, which results in a seaward flow of estuarine water near the surface and landward flow of dense water near the bed. This is known as the gravitational circulation (Geyer and MacCready, 2014). Depending on the estuary´s geometry and tidal forcing, strain-induced periodic stratification (SIPS) can occur with stratification during ebb and mixing during flood (Simpson et al., 1990). This tidal asymmetry enhances estuarine circulation (Jay and Musiak, 1994) and has been referred to as tidal straining circulation (Burchard et al., 2011; Geyer and MacCready, 2014) or eddy viscosity – shear covariance ~~(ESCO, . Other drivers include e.g.~~ (ESCO, Dijkstra et al., 2017). Salt transport is also controlled by e.g. lateral momentum advection (Burchard et al., 2011) ~~or~~ and estuarine convergence (Ianniello, 1979; Burchard et al., 2014). The strength of salt transport mechanisms depends on the water depth and it is therefore expected that channel deepening affects saltwater intrusion (Andrews et al., 2017).

Studies have been conducted in estuaries worldwide to try to quantify the impact of changes in topography, i.e., channel deepening or widening, on saltwater intrusion. In recent studies, numerical models with different topographies have been used to examine mixing and transport processes in estuaries before and after implementing engineering measures. Among others, such investigations have been conducted for the San Francisco estuary, US (Andrews et al., 2017), the Hudson River estuary, US (Ralston and Geyer, 2019), the Danshui River estuary system, Taiwan (Liu et al., 2020), the Seine estuary, France (Grasso and Le Hir, 2019), and the Ems estuary, Germany (van Maren et al., 2015).

Generally, it was found that a deepening of the river channel is associated with a landward shift of the brackish water zone. Several studies explain the increase in landward salt transport with an increase in the estuarine circulation and a decrease in vertical mixing processes, which occur due to the larger water depths (Grasso and Le Hir, 2019; Andrews et al., 2017; van Maren et al., 2015). In the case of the Danshui river estuary, some channels have been deeper in the predevelopment state, which goes along with increased gravitational circulation and a further ~~upstream~~landward limit of the ~~salinity~~saltwater intrusion in the predevelopment state (Liu et al., 2020). All the other above-mentioned estuaries are deeper in the present state. Grasso and Le Hir (2019) investigated key estuarine processes in the Seine estuary in 1960 and 2010 and detected a relative increase in gravitational circulation and stratification. This caused an up-estuary shift of the salinity front and changed the response of saltwater intrusion to tides and discharge. Ralston and Geyer (2019) examined the Hudson River estuary in the present state and the predevelopment state. They detect an increase in saltwater intrusion and stratification, but only a minor change in estuarine circulation and no change in the response of saltwater intrusion to river discharge. The authors conclude that dredging in the Hudson did not significantly change estuarine exchange processes.

In most of the abovementioned studies, a numerical model of the respective estuary in the present state was set up and calibrated. Different model topographies were subsequently inserted to represent earlier states of the estuary (Ralston and Geyer, 2019; Grasso and Le Hir, 2019; Liu et al., 2020). Models representing earlier system states of the estuary were not calibrated. However, differences in bed roughness are expected to occur between the system states due to sediment redistribution and changes in bed forms, which are usually not resolved in the models. Van Maren et al. (2015) calibrated models of the Ems estuary for different system states and obtained significantly larger roughness values with historical bathymetries compared to the present state. This is attributed to the observation that sediment in the Ems estuary has successively become finer in the last decades. The authors conclude that changes in bed roughness can strongly contribute to shifts in hydrodynamics and transport processes. In addition to shifts in bed roughness, the resolution of data which are used to generate model topographies may differ for the system states, ~~with~~which can have an effect on form drag. ~~Thus, the system behaviour at different points of time~~When setting up models with different topographies, individual calibration of each model might thus be ~~better represented with individually calibrated models~~advantageous.

In the Weser estuary, no model-based examinations have yet been conducted to examine the effect of anthropogenic measures on saltwater intrusion. Instead, saltwater intrusion and influencing parameters have been tracked by measurements and ~~attempts have been made~~it was attempted to separate the impact of different factors (Krause, 1979; Grabemann et al., 1983). However, many factors affect saltwater intrusion on different time scales and it has ~~therefore~~thus not been possible to isolate the impact of topography variations (Grabemann et al., 1983). Within each tidal cycle, the position of the brackish water zone shifts by more than 15 km along the navigation channel of the Weser (Kösters et al., 2014). Changes in tidal components, meteorological conditions, long-term variations of the salinity of the North Sea, and variations in discharge also affect the position of the brackish water zone (Grabemann et al., 1983). Due to variations in discharge, the tidally averaged ~~salinity~~saltwater intrusion shifts by more than 20 km, whereby the impact of discharge variations is larger for low-discharge ~~conditions~~ than high-discharge conditions (Kösters et al., 2014).

This study aims to systematically quantify saltwater intrusion in a real tidal estuary in different system states and to determine to what degree anthropogenic measures, in particular deepening measures, impact saltwater intrusion in the estuary. As an example, we studied the Weser estuary in the German Bight and set up numerical model simulations in four different system states (1966, 1972, 1981, 2012). In contrast to most previous studies, we individually calibrated each model and conducted simulations with realistic and with idealized forcing. In this paper, we describe the model setup and simulation results. We discuss the methodology, the importance of calibration for the model-based examination with different model topographies, and the effect of channel deepening on processes governing saltwater intrusion.

2 Study site: the Weser estuary

2.1 Geomorphology and hydrology

The Weser estuary, located in Northern Germany, is of high ecological and economic importance. It is divided into two sections: the Lower Weser and the Outer Weser (see Fig. 1). The Lower Weser stretches from the tidal weir at Bremen-Hemelingen (km 0, the tidal limit) to Bremerhaven (km 66.7). The funnel-shaped Outer Weser starts from Bremerhaven and

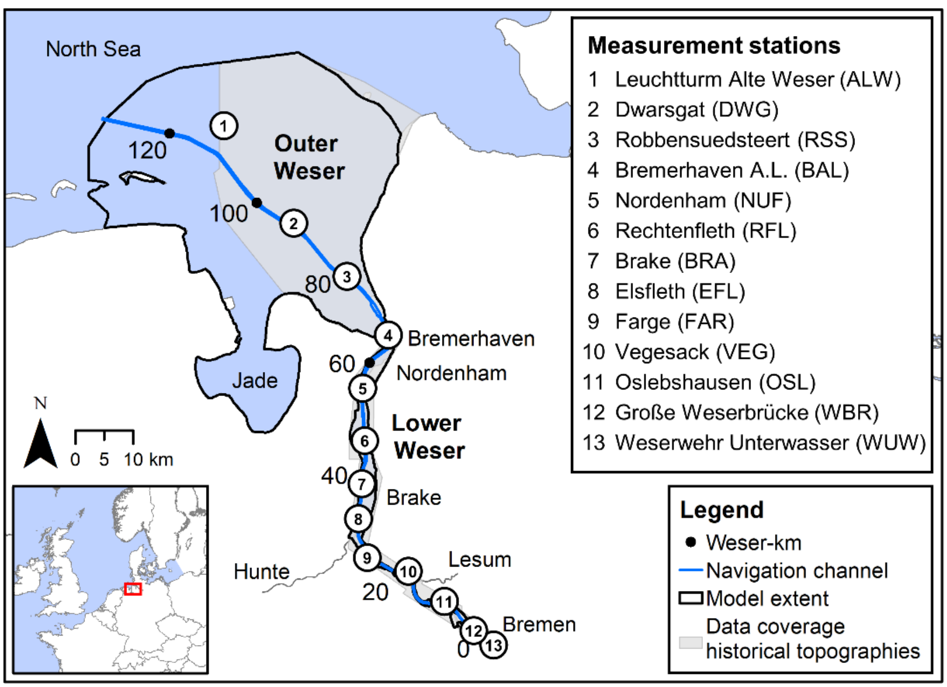

~~**Figure 1. Map of the model area and distance along the navigation channel from the tidal weir at Bremen (Weser-km) with data coverage for historical topographies displayed in grey.**~~

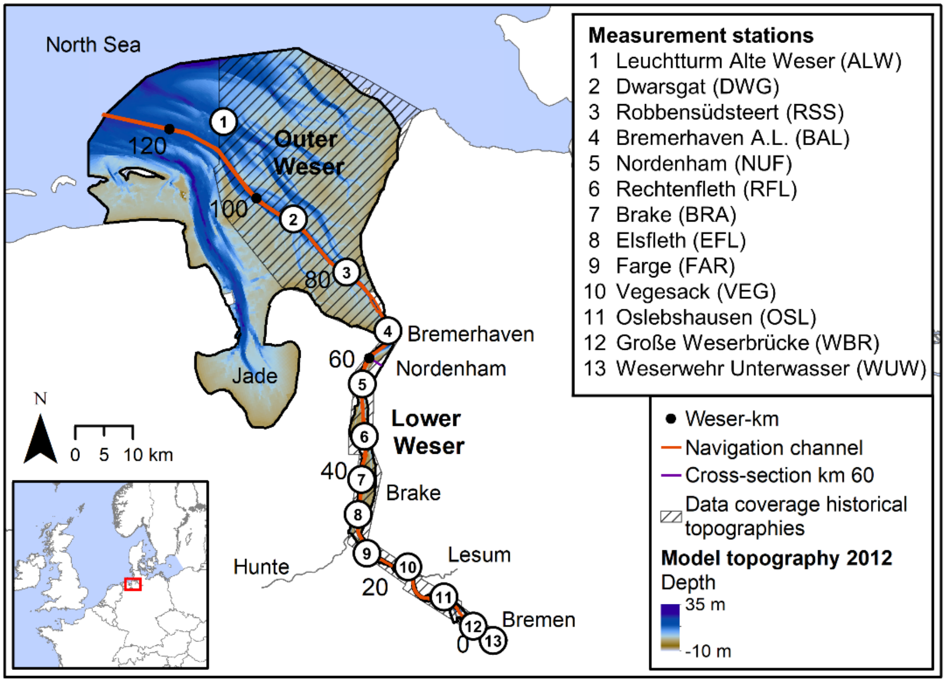

Figure 1. Map of the model area with the model topography 2012 displaying measurement stations and the distance along the navigation channel from the tidal weir at Bremen (Weser-km). The hatched area shows the data coverage for historical topographies.

opens towards the North Sea (Weser-km 126). The estuary is an important shipping channel, providing access to the container terminal of Bremerhaven, the port of Bremen, and several smaller ports. In 1941–2015, the mean annual discharge, measured at station Intschede, was 321 m³ s^{-1} with high seasonal variability (NLWKN, 2018). In the same period, the mean low discharge (mean value of the smallest discharge of each year 1941–2015) was 116 m³ s^{-1} and the mean high discharge (mean value of the largest discharge of each year 1941–2015) was 1200 m³ s^{-1} (NLWKN, 2018).

The semidiurnal tidal wave from the North Sea propagates through the Weser estuary in about three hours. At the northern part of the Outer Weser, the tidal range is 2.8 m. On its way through the estuary, it increases to 3.8 m near Bremerhaven due to estuarine convergence, slightly decreases between Weser-km 50 and ~~km~~ 30, and increases to 4.1 m near Bremen. In most stretches of the navigation channel of the Lower and Outer Weser, ebb currents are slightly stronger than flood currents. Flood currents dominate in some stretches, such as Weser-km 80–95 (Lange et al., 2008).

Before mixing with seawater, the river Weser has an initial salinity of about 0.5 psu as a caustic potash solution is discharged further upstream. The mean position of the 2 psu isohaline is located at Weser-km 45 at the reversal from flood to ebb (high water slack) and Weser-km 60 at the reversal from ebb to flood (low water slack) (Lange et al., 2008).

2.2 Historical development

The topography of the Weser estuary has been strongly altered through river deepening and correction measures since the end of the 19th century. The main objective of these measures was to establish and maintain a continuous shipping route with sufficient depth and width for ships of increasing size to pass through (Wetzel, 1988).

Since 1960, three major deepening measures have been conducted. The Outer Weser was modified in 1969–1971 to create a continuous depth of nautical chart datum 'Seekartennull' (SKN) -12 m and in 1998–1999 to increase the depth to SKN -14 m

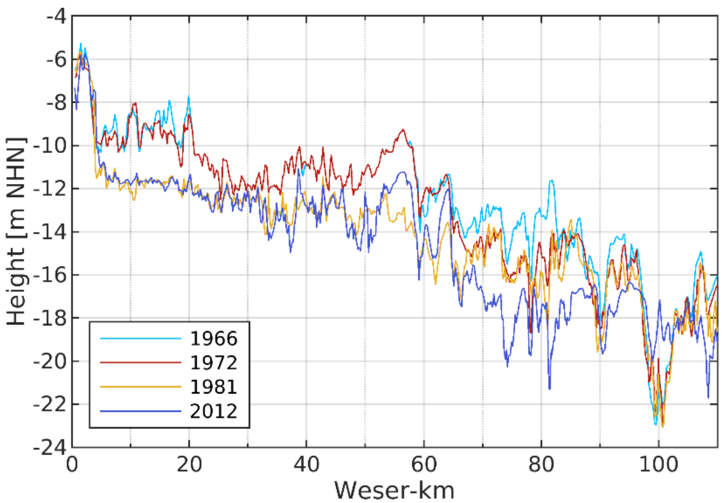

~~**Figure 2. Height along the navigation channel (200-300 m width) in the Weser estuary in different years, based on model topographies.**~~

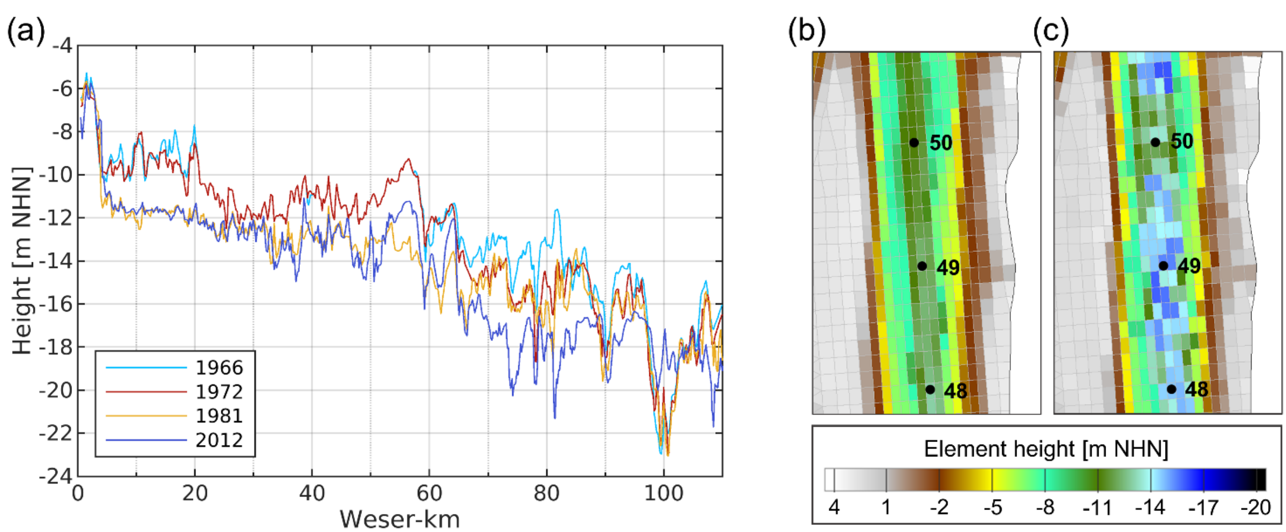

Figure 2. Height along the navigation channel (200-300 m width) in the Weser estuary in different years, based on model topographies (a). Element height in a section of the Lower Weser of model topographies 1972 (b) and 2012 (c).

(Lange et al., 2008; Wetzel, 1988). Engineering measures at the Lower Weser were conducted in 1973–1978. Thereby, the stretch between Brake (Weser-km 39) and Bremen (Weser-km 0) was deepened to nautical chart datum SKN -9 m, and the stretch between Bremerhaven and Nordenham to SKN -11 m (Lange et al., 2008; Wetzel, 1988). Starting in 1982, additional groynes were constructed in the Lower Weser to regulate the flow further. The mouth of the Ochtum tributary was relocated in 1972–1976, and the mouth of the Hunte tributary in 1979. Moreover, regular dredging measures for maintenance were conducted in the navigation channel (Lange et al., 2008). The bathymetry height along the navigation channel in the four system states is depicted in Fig ~~2~~2a.

3 Methods

We built numerical models of the Weser estuary in four system states: 1966, 1972, 1981, and 2012. A simulation of one hydrological year was conducted for each model with realistic forcing to hindcast hydrodynamics and saltwater intrusion (‘hindcast study’). Results from previous calibration runs with respective topographies were used as initial conditions and a spin-up time of four weeks was applied. Additionally, simulations of each system state, but with identical forcing, were conducted and analysed for one spring–neap cycle (after six weeks spin-up time) so that the impact of topography changes and roughness changes could be individually evaluated (‘scenario study’). ~~In all simulations, salinity along the navigation channel (see Fig. 1) was analysed and the location of the salinity front, which was defined as the vertically averaged 5 psu isohaline, was calculated.~~

3.1 Description of the numerical model

Numerical simulations are based on UnTRIM^2 (Casulli, 2008). UnTRIM^2 solves the Reynolds-averaged Navier Stokes equations, the continuity equation, and transport equations based on a semi-implicit finite volume / finite difference approach to calculate current velocities, surface elevations, and tracer concentrations (Casulli and Walters, 2000). The equations are solved on a horizontally unstructured grid with vertical z-layers of 1 m thickness. The model considers 3D hydrodynamics, daily freshwater discharge from the Weser, and the transport of salinity and heat. Vertical turbulent mixing was estimated with a two-equation k-ε model; horizontal mixing was modelled with a constant viscosity (0.1 $m^2 s^{-1}$) and diffusivity (0.1 $m^2 s^{-1}$) in all simulations. UnTRIM^2 was coupled with the sediment transport model SediMorph (BAW, 2002), but only to calculate bottom roughness. ~~For simplicity, we~~Sediment transport was neglected ~~sediment transport~~ in this study. The model is well-suited to simulate flows in estuaries, as the algorithm accurately preserves mass where wetting and drying occurs (Casulli, 2008). For example, it has been used to simulate flows in San Francisco Bay (Andrews et al., 2017), the German Bight (Hagen et al., 2021b; Rasquin et al., 2020), and the Weser Estuary (Kösters et al., 2014).

3.2 Model topographies

The model area includes the Lower Weser, the Outer Weser, and the adjacent Jade (see Fig. 1). Tributaries of the Weser and their discharge are not represented, as ~~topographical~~bathymetric and hydrographic data of the tributaries are not available for all system states. The same unstructured orthogonal calculation grid was used in all models. It contains cells of different sizes, arranged to increase the resolution in areas of interest. Cell spacing in the navigation channel is 50–250 m.

Model topographies were created by interpolating respective topographical data on the calculation grid, smoothening transitions, and correcting essential landscape features. The accuracy of the data sets differs depending on the quality and density of the original data. The model topography of 2012 is based on ~~elevation data from~~ airborne laser scanning (ALS) for flat areas, multibeam ~~echosounder~~echo-sounding for deep channels, and single-beam echo-sounding for shallow areas. Older bathymetries are mostly based on single-beam echo-sounding measurements ~~and laser scanning flights. Model topographies of the other system states are based on~~. For most of the Outer Weser, topographical maps at a scale of 1:20.000 containing tracks with 70-200 m distance were used. For the Lower Weser, measurements along cross-sections with 125 m longitudinal spacing were used. Topographical measurement data were not available for all regions for each time period. For example, historical ~~maps with diverse land and hydrographic surveying data. These maps have been~~data for the northern Outer Weser were only available from nautical charts of 1970 with lower data density. With temporal and spatial interpolation, considering deepening measures, all data were compiled to historical topographies of the Lower and Outer Weser (see Fig. 1, ~~grey~~hatched area) in different historical system states (BAW, 2020, 2021). We interpolated the ~~topographical~~ bathymetric data from 1966, 1972, and 1981 on the computational grid preserving the wet volume ~~and~~, which ensures that the water volume in the model agrees exactly with the average depths of the bathymetric data. We then filled the remaining area of the North Sea and Jade with ~~bathymetrical~~bathymetric data from 2012. Subsequently, we corrected important landmarks and structures such as summer dikes, side channels, constructions, and the transition between Outer Weser (historical ~~topographic~~bathymetric data) and Jade (~~topographic~~bathymetric data of 2012) in the case of the model topographies 1966, 1972, and 1981.

~~Please note that~~ Due to the differences in temporal and spatial data coverage, ~~which determines~~ the ~~models'~~ quality and level of ~~details, varies for the different decades. For the generation~~detail of the ~~historical topographies, data~~model topographies differs. For example, bedforms such as dunes landwards of Weser-km 55 (Lange et al., 2008) are represented in the model topography of 2012 as variations in depths (see Fig. 2c). Historical recordings were ~~scarcer and~~ less detailed ~~than the present state. Therefore, the resolution of small-scale features such as bedforms in the different~~, i.e. model topographies ~~is~~of 1966, 1972, and 1981 do generally not ~~directly comparable. With less representation of small-scale features in historical~~contain information on bedforms. Hence, the older topographies ~~, the bathymetry is~~ are smoother ~~and the roughness effect of varying topography represented in the grid is lower. This influences the model results. As an indicator for the resolution of the different model topographies, we evaluated the depth variation along the estuary in the different setups. We extracted depth values h_1 to h_n at n defined points along a transect along the navigation channel (every 50 m). Then, we calculated the average depth variation Δ_h between adjacent points with~~

$$\cancel{\Delta_h = \frac{\sum_{i=1}^{n-1} |h_{i+1} - h_i|}{n-1}.} \qquad \cancel{(1)}$$

~~Our results show that between Bremen and Nordenham (Weser-km 55.8), the depth variation in the 2012 model is almost twice as high as in the historical systems states (see Table 1). This indicates a higher resolution of the original topographic data with a representation of small-scale features and a higher form drag. Minor differences in depth variation do also occur between the individual model topographies. To~~than 2012 (see Fig. 2b). We account for the different resolutions of the underlying bathymetric data and their effect on form drag~~, we~~ by individually ~~calibrated~~calibrating the models of each system state with the respective topographies (see ~~Section~~Sect. 3.~~4~~6).

~~**Table . Depth variation (see Eq. (1)) along a transect in different system states between Bremen and Nordenham (Weser-km 1.5–55.8) and between Nordenham and the North Sea (Weser-km 55.8–126).**~~

	~~1966~~	~~1972~~	~~1981~~	~~2012~~
~~Along Weser-km 1.5-55.8 (in m)~~	~~0.15~~	~~0.15~~	~~0.16~~	~~0.29~~
~~Along Weser-km 55.8-126 (in m)~~	~~0.10~~	~~0.11~~	~~0.12~~	~~0.12~~

3.3 Initial sediment distribution

We prescribed an identical initial sediment distribution in all models based on diverse sediment samples as described in Milbradt et al. (2015). The sediment distribution represents the system state 2012; data from previous years were additionally used at locations with insufficient data coverage. The distribution comprises eight fractions of sediments: very coarse sand, coarse sand, medium sand, fine sand, very fine sand, coarse silt, medium silt, and fine silt. ~~Even though it is very likely that the sediment distribution in the Weser estuary has changed between the system states 1966, 1972, 1981, and 2012, we decided to~~We use the same initial sediment distribution in all models as historical data ~~are scarce. We assume that the effect of this simplification is small~~to suitably represent changes in sediment distribution over time were not available. In the models, the initial sediment distribution is used for roughness calculation based on sediment type and bedform prediction (see ~~Section~~Sect. 3.6).

3.4 Model forcing

As boundary conditions, we prescribed time series for salinity, temperature, and water level at the seaward boundary to the North Sea. ~~Furthermore, we~~We also provided salinity, temperature, and discharge of the Weser at the landward boundary. The hindcast study aimed to represent the system states as realistically as possible. Measurement values were retrieved from the Waterways and Shipping Authorities Bremerhaven, Bremen and ~~Hann.~~ Hannoversch Münden and time series were constructed by linear interpolation between observations. Measured values were available for most parameters, but not for water level and salinity at the seaward model boundary in the North Sea in 1966, 1972, and 1981~~.~~ and for salinity and temperature at the landward boundary in 1966. For the water level however, historical records for tidal high and low water levels were available for the station 'Leuchtturm Alte Weser' (ALW, see Fig. 1) close to the model boundary. Thus, we generated a synthetic time series of 1965–2012 by reconstructing the astronomical tide at station ALW, fitting the signal to measured high water and low water values and inducing a phase shift and amplitude amplification to account for the distance of the station to the model boundary. ~~The synthetic time series was used for all models for the sake of consistency, even though measured records of water level at ALW would have been available for the hindcast model of 2012.~~ Salinities at four positions along the open boundary were approximated utilising neural networks of two layers (55 and 11 neurons) with a Levenberg–Marquardt algorithm. For each position, 100 networks were trained with salinity values of 1996–2016, which were extracted from a validated model of the German bight, the Easy GSH model (Hagen et al., 2021a). As reference data, the tidal range and tidal mean water level at station ALW, salinity records at Helgoland station (Wiltshire et al., 2008), and the discharge of the Weser and Elbe were used. Subsequently, the correlation of network results and the extracted target salinity values were calculated and the best network for each position was selected. With the selected networks, salinity at each position was predicted for all system states (1965–2012). For evaluation of the ~~hindcast model 2012, consistent boundary values would have been available from measurements or from the aforementioned Easy GSH model. However, we stuck to the~~ performance of neural networks ~~to ensure consistency~~, a skill estimator was applied according to Murphy (1988), implemented in the form suggested by Ralston et al. (2010).

$$MSS = 1 - \frac{\sum_{i=1}^{N}(X_{sim} - X_{obs})^2}{\sum_{i=1}^{N}(X_{obs} - \bar{X}_{obs})^2} \qquad (2)$$

The Murphy Skill Score MSS compares the squared error between approximated values X_{sim} and observed values X_{obs} with the ~~models of different system states. Moreover,~~squared error between observation values and mean of observation values at each time step. It evaluates the prediction of the neural networks in comparison to the mean observation values. If the $MSS < 0$, the mean observation value is better than the prediction of the neural network and vice versa. The Murphy Skill Score of the selected networks ranges between 0.34 (western model boundary) to 0.7 (eastern model boundary), indicating that prediction with the neural networks was effective. Boundary values for salinity and temperature at the landward boundary for the hindcast model 1966 were reconstructed. For salinity, a relationship between discharge and salinity was derived based on measured data from 1967–1968, where the amount of potash discharging can be assumed to be similar to 1966. Salinity values for the hydrological year 1966 were calculated based on measured discharge values with

$$S_{river} = 6 * 10^{-7} \frac{psu}{m^6\, s^{-2}} * Q^2 - 0.0017 \frac{psu}{m^3\, s^{-1}} * Q + 2.0759\, psu, \qquad (\cancel{2}3)$$

where S_{river} is salinity and Q is discharge. For temperature, measured values of 1968 were used instead of 1966, as the variations over the years were assumed to be similar and temperature is only of secondary importance in this study.

In contrast to the hindcast study, we used identical boundary values in all simulations for the scenario study. The synthetic time series of the hindcast model 2012 was used for water level at the open boundary. For all other parameters, cross-scenario boundary values were generated; representing an average of the four system states (see Table ~~2~~1).

Table 1. Boundary values in hindcast study (realistic forcing) and scenario study (identical forcing). In each study, simulations of system state 1966, 1972, 1981, and 2012 were conducted. ~~For the hindcast model of 1966, no measured values for salinity and temperature in the Weser were available. Therefore, salinity values were approximated based on the relationship to discharge (see Eq. (2)); temperature values were replaced with values of 1968, the closest year with available records.~~

Boundary condition	Hindcast study	Scenario study
North Sea water level	Synthetic time series (of respective year)	Synthetic time series (of 2012)
North Sea salinity	Time series generated with neural networks	28.7 psu
North Sea temperature	Time series constructed from observations	15.5 °C
Weser discharge	Time series constructed from observations	300 m³ s^{-1}
Weser salinity	Time series constructed from observations	1.2 psu
Weser temperature	Time series constructed from observations	19.9 °C

3.5 Analysis methods

Model results were analysed by ~~evaluation of~~calculating tidal characteristic values, which describe the tidal curve and facilitate characterization of the system's behaviour and comparison between simulations (Lang, 2003). Thus, for example, the tidal range and the minimum, mean, and maximum salinity per tidal cycle were calculated in each scenario and compared.

In addition, the position of the brackish water zone was calculated for all model results by determining the position of the ~~vertically averaged~~ 5 psu and 20 psu isohaline along the navigation channel (see Fig. 1) based on the tidal mean of the vertically averaged salinity~~ per tidal cycle~~. The saltwater intrusion length was defined as the distance from the estuary mouth (Weser-km 126.2, see Fig. 1) to the ~~mean~~ 5 psu isohaline along the navigation channel. ~~Further,~~In order to identify processes driving the saltwater intrusion the following analysis methods have been applied.

3.5.1 Regression analysis

The effect of discharge on the saltwater intrusion length was quantified by means of a regression analysis based on data from the hindcast simulations. Saltwater intrusion was calculated for each tidal cycle within the respective hydrological years and discharge conditions were assigned. Data points were then sorted into 50 m³ s^{-1} bins of discharge between 150–400 m³ s^{-1} and 100 m³ s^{-1} bins between 400–1,100 m³ s^{-1} and averaged to reduce the effect of additional factors and outliers. If fewer than 10 entries were available for a category, these entries were excluded. Based on the resulting average intrusion length for the specified discharge categories, multiple nonlinear regression with interaction effects was performed with the Levenberg–Marquardt algorithm to obtain trends of the form

$$L^{*} = kQ^{m} \, , \qquad (4)$$

~~potential~~with saltwater intrusion length L^{*}, factor k, discharge Q, and exponent m. The analysis was repeated without data aggregation to examine the method's validity.

3.5.2 Salt flux decomposition

We decomposed the total salt flux F_{tot} into three components: barotropic flux F_{bf}, estuarine exchange F_{exf}, and tidal pumping flux F_{tp}. The method is based on the decomposition analysis of sediment fluxes of Becherer et al. (2016). We focused our analysis on the brackish water zone and have chosen a cross-section in the Lower Weser (Weser-km 60, see Fig. 1) to carry out the decomposition. We first interpolated our data on a σ-layer grid with M=50 equidistant layers. Then we calculated the temporal average of salinity s and horizontal velocity u at σ-layers with

$$\langle X_\sigma \rangle_t = \left[\int_{t=0}^{T} h_\sigma(t)\ dt\right]^{-1} \int_{t=0}^{T} X_\sigma(t)\, h_\sigma(t)\, dt \qquad (5)$$

Where X is the respective quantity, h is the height of the σ-layer, and T is the analysis period. Temporal averages are represented by angle brackets. Becherer et al. use a moving average window to track effects of variable forcing on the flux components. As the simulations are run with constant river discharge as forcing, we can simply average over the entire analysis period of the scenarios (one spring-neap cycle). We calculated deviations from the mean, indicated by curly brackets, with

$$\{X_\sigma\}_t(t) = X_\sigma(t) - \langle X_\sigma \rangle_t \qquad (6)$$

Vertical averages were calculated according to

$$\langle X \rangle_\sigma = \frac{1}{M} \sum_{\sigma=1}^{M} X_\sigma \qquad (6)$$

From the temporal and vertical averages and deviations, we determined the salt flux components and integrated over the cross-section's width W.

$$F_{tot} = \langle D \rangle_t \langle \langle su \rangle_t \rangle_\sigma = \underbrace{\int_{w=0}^{W} \langle D \rangle_t \langle s \rangle_{t,\sigma} \langle u \rangle_{t,\sigma}\, dw}_{F_{bf}} + \underbrace{\int_{w=0}^{W} \langle D \rangle_t \langle \{\langle s \rangle_t\}_\sigma \{\langle u \rangle_t\}_\sigma \rangle_\sigma dw}_{F_{exf}} + \underbrace{\int_{w=0}^{W} \langle D \rangle_t \langle \{s\}_t \{u\}_t \rangle_{t,\sigma} dw}_{F_{tpf}} \qquad (7)$$

The barotropic flux F_{bf} contains residual barotropic flows due to river discharge, barotropic ebb-flood asymmetries, and wind stress. The vertical exchange flow F_{exf} indicates the estuarine circulation and the tidal pumping flux F_{tp} indicates upstream transport by the correlation of salinity and velocity fluctuations (Becherer et al., 2016).

3.5.3 Potential energy anomaly ~~Φ was evaluated.~~

According to Simpson (1981), the potential energy anomaly Φ is the energy required to homogenise the water column with given density stratification instantaneously. Burchard and Hofmeister (2008) define it as

$$\Phi = \frac{1}{D}\int_{-H}^{\eta} gz(\bar{\rho}-\rho)\,dz;\ \bar{\rho} = \frac{1}{D}\int_{-H}^{\eta}\rho\,dz\,, \qquad (~~3~~8)$$

where H is the mean water depth, η is the water level elevation, $D = \eta + H$ is the actual water depth, g is the gravitational acceleration, and ρ is the density. Thus, an increase in potential energy anomaly indicates an increase in stratification~~.~~ assuming a constant water level.

3.6 Calibration and validation

Models of each system state were calibrated in two steps by adjustment of the roughness settings: first, tuning of a form roughness predictor, and second, definition of an additional roughness in the Lower Weser. ~~Simulation~~The simulation time for each system state was ~~one spring -neap cycle within the respective year.~~ four weeks. Bottom roughness ~~is~~ in our models is described by Nikuradse´s effective roughness coefficient k_s, which relates to the bed roughness length z_0 with $z_0 \simeq k_s/30$ (Malcherek, 2010)~~. It is composed~~. In nature, roughness can be seen as the sum of grain ~~roughness,~~and form related roughness~~, and additional roughness.~~. The sediment transport model SediMorph, which is coupled with the hydrodynamic model UnTRIM², calculates the grain roughness $k_{s,grain}$ at each element from the prescribed sediment distribution with $k_{s,grain} = 3d_m$, where d_m is the mean grain size. ~~Additionally, form~~Form roughness is estimated at each time step of the simulation based on ~~present sediments and the respective~~sediment properties, water depth, and velocity, according to van Rijn (2007). Calibration factors, which determine the prevalence and importance of bedforms (ripples, mega ripples, dunes), ~~can be specified and~~ were varied in the calibration ~~runs~~ to optimise the agreement between simulated and observed ~~and simulated~~ water levels~~. As the roughness~~ , if available (system state 2012), high water and low water values (all scenarios), and the tidal range (all scenarios). The effect of dunes could not be reliably modelled with the predictor ~~underestimated roughness in the Lower Weser, we defined~~but had to be prescribed as an additional roughness ~~of up to 0.36 m~~ landwards of Weser-km 55~~ to represent damping of the tidal wave, with some variation amongst the models. Landwards of Weser-km 55, pronounced dunes and ripples are positioned , which are not explicitly resolved in the models' calculation grid. Moreover,~~. The additional ~~damping was required~~roughness also compensates model effects, such as due to the omission of the Weser's tributaries~~ of the Weser.~~. Tributaries typically ~~have~~ dampen the tidal wave through low water depths and high energy dissipation rates. The additional roughness increases from Weser-km 55 towards Weser-km 26 and decreases afterwards again. In this way, damping of the tidal wave could be well represented. Roughness as calculated by the numerical model (effective bed roughness) along the navigation channel is described in Table 2. For each model, different roughness settings were determined. ~~Thus, when tributaries are omitted, the models tend to underestimate energy dissipation, which can be outbalanced through an increase~~While the estimated form roughness is in the range of 0.01 to 0.04 m, the maximum additional roughness ranges from 0.22 m (system state 2012) to 0.36 m (system state 1981). The mean RMSE of tidal range in ~~bottom roughness.~~scenarios 1966, 1972, and 1981 improved by almost 50 % after adjustment of the roughness settings by individual calibration (see Table 2).

In other estuaries, changes~~For each model, different roughness settings were determined. Differences are caused by natural variations~~ in sediments and bedforms ~~between the system states, which~~ were observed over time. For example, dredging induced fine sediment accumulation in the Ems (Winterwerp et al., 2013; van Maren et al., 2015) and reduced drag associated with bedforms in Columbia river (Jay et al., 2011), both contributing to lower friction and an amplification of tides. There are no data to assess whether there have been comparable changes in sediment inventory in the Weser estuary. But the height of bedforms will almost certainly have changed with changing water depths. Such changes are not represented in ~~the~~our models ~~due to the lack of historical sedimentological data, and by~~, which could explain to some extent differences between scenarios. In addition, effects induced by the different resolutions of the original ~~topographic~~bathymetric data~~. The least additional roughness was required in the model of system state 2012, where the resolution of original topographic data was comparatively high~~ (see ~~Table 1).~~Sect. 3.2) are balanced out through roughness calibration. To some extent, dunes are depicted in the numerical grids – if present in the bathymetric data. In the examined years prior to 2012 bathymetric data almost did not resolve dunes. This has an effect on depth variation in the model topographies and the associated form drag. The lower depth variation in the older model topographies is compensated by defining a higher additional roughness. The largest additional roughness ~~in the area of Lower Weser~~ was required in the model of system state 1981 (see Table ~~3~~1). The model topography includes the deepening of the Lower Weser to SKN -9 m~~,~~, in 1973–1978 (see Sect. 2.2), which ~~was undertaken shortly before 1981 (see Section 2.2). The deepening~~ led to ~~a volume increase, larger water depths, and an increase~~strong changes in tidal ~~range~~dynamics. The model seems to overestimate this effect, possibly due to the ~~coarse~~limited model resolution and omission of tributaries~~, if not~~. This could be outbalanced by the additional roughness. ~~The mean RMSE of tidal range in scenarios 1966, 1972, and 1981 decreased by almost 50 % after adjustment of the roughness settings by individual calibration~~Possible tests to further evaluate the effect of the resolution of bathymetric data could include smoothing the 2012 model topography to be comparable to historical topographies and evaluating the effect on calibration results. Alternatively, the low resolution of historical bathymetric data could be compensated by adding artificial surface irregularities, which represent the depth variation due to e.g. sand waves, as implemented by Hubert et al. (2021).

Table 2~~. Effect of the calibration~~. Effective bed roughness along the navigation channel of the Weser estuary (see Fig 1) and RMSE of ~~roughness settings on results of~~the tidal range for the individually calibrated models. For 1966, 1972, and 1981, results are compared to ~~results of the~~ respective ~~models~~calculations with roughness settings of 2012~~. Effective bed roughness was evaluated along the navigation channel (see Fig. 1).~~ (before individual recalibration).

		1966	1972	1981	2012
~~Change in effective~~Effective bed roughness	Along Weser-km 1.5-55.8	0.20 m (+25 %)	0.18 m (+14 %)	0.25 m (+56 %)	0.16 m
	Along Weser-km 55.8-126	0.015 m (+184 %)	0.019 m (+272 %)	0.010 m (+84 %)	0.006 m
~~Change in~~ RMSE of tidal range	At stations with available measurements for all scenarios	0.17 m (-48 %)	0.19 m (-46 %)	0.19 m (-44 %)	0.09 m

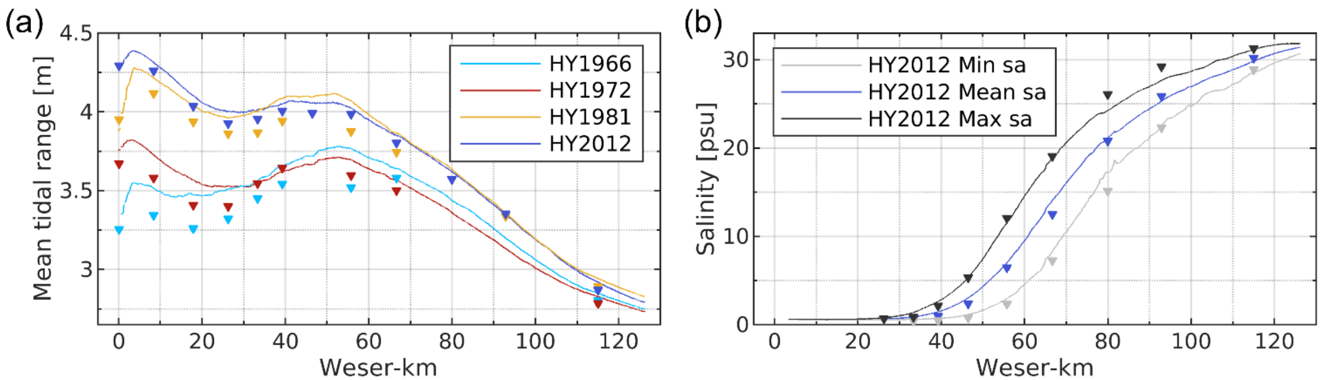

~~**Figure 3. Mean tidal range along the navigation channel of the Weser estuary (see Fig. 1) in hindcast models of 2012, 1981, 1972, and 1966 (a) and vertically averaged mean, minimum, and maximum salinity per tide (average) in hindcast model HY2012 (b). Simulation results (lines) are compared to measured values (triangles), averaged over the same period.**~~

Figure 3. Mean tidal range along the navigation channel of the Weser estuary (see Fig. 1) in hindcast models of 2012, 1981, 1972, and 1966 (a) and vertically averaged mean, minimum, and maximum salinity per tide (average) in hindcast model HY2012 (b). Simulation results (lines) are compared to measured values (triangles), averaged over the same period.

The models were subsequently validated by extending the calculation time to one hydrological year (plus the preceding four weeks to allow for a model spin-up) and comparing model results to measurements. One hydrological year is ~~defined as~~ the time between November 1st of the previous year and October 31st of the respective year (DIN 4049-1:1992-12). The tidal range in the Lower Weser was slightly overestimated in the hindcast models (see Fig. 3a), but overall well reproduced with a mean RMSE of 0.166 m (1966), 0.114 m (1972), 0.169 m (1981), and 0.153 m (2012), averaged over stations along the navigation channel with available measurements for all scenarios. Measured values of water level and salinity only covered system state 2012. The mean RMSE for the comparison of modelled and observed water levels in ~~hindcast model~~ 2012 was 0.~~224~~22 m ~~for water level~~, averaged over all measurement stations (see ~~Figure~~Fig. 1). An overall bias of 5 cm indicated a slight, consistent overestimation of water levels. ~~Salinity~~A visual inspection of observed and modelled water levels suggested a correct phasing of tides, which is corroborated by the low RMSE. Saltwater intrusion was slightly overestimated, with higher computed values than measured values in Lower Weser (see Fig. 3b). The ~~intertidal~~intratidal variation in Weser-km 60–100 was slightly underestimated, with higher minimum salinity and lower maximum salinity per tide. The mean RMSE in hindcast model 2012 was 1.~~42~~24 psu for mean salinity, averaged over all stations with available measured values. Overall, the magnitude and dynamics of saltwater intrusion were reproduced well in the hindcast model 2012. It is expected that the model performance will be similar for the other system states.

4 Results

4.1 Natural variability of saltwater intrusion in the Weser estuary

~~As described above,~~In order to give an idea of temporal variation of salinity in the Weser estuary ~~is subject to strong variations on different time scales (see Introduction). We studied salinity intrusion in~~ measurement data of the hydrological year 2012 ~~based on measurement data~~are shown in Fig. 4. In each semi-diurnal tidal cycle, the 5 psu isohaline moves up- and downstream by almost 20 km (see Fig. 4a). It is located about 2 to 3 km further landward during spring tide compared to neap tide. The mean position of the 5 psu isohaline per semi-diurnal tidal cycle shifts by more than 30 km within the ~~hydrological~~ year ~~2012~~. A major seaward shift occurs in December and January, where the isohaline moves from Weser-km 40~~–~~ to Weser-km 73. This is induced mainly by an increase in discharge from 100 m³ s^{-1} to 1000 m³ s^{-1}.

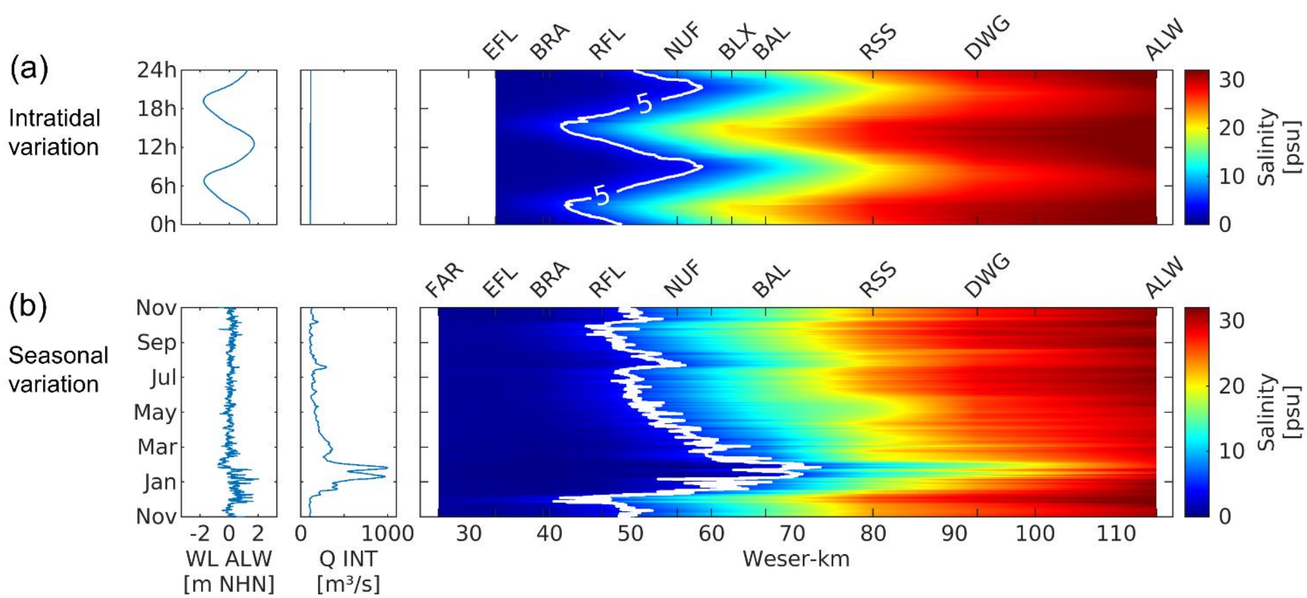

~~**Figure 4. Intratidal and seasonal variation of saltwater intrusion in the Weser estuary. The water level at station Leuchtturm Alte Weser (ALW), discharge at station Intschede (INT), and salinity along the navigation channel of the Weser estuary are displayed on different time scales. Salinity values were interpolated linearly between measurement stations with available measurements along the navigation channel. The 5 psu isohaline is displayed in white. On top, salinity variation within one day, September 1st, 2012, is depicted (a). Below, variation within the hydrological year 2012 of the mean salinity per tidal cycle is depicted (b). We applied a moving median filter to the water level data in (b) to show the seasonal variation (filter size 12h 25min).**~~

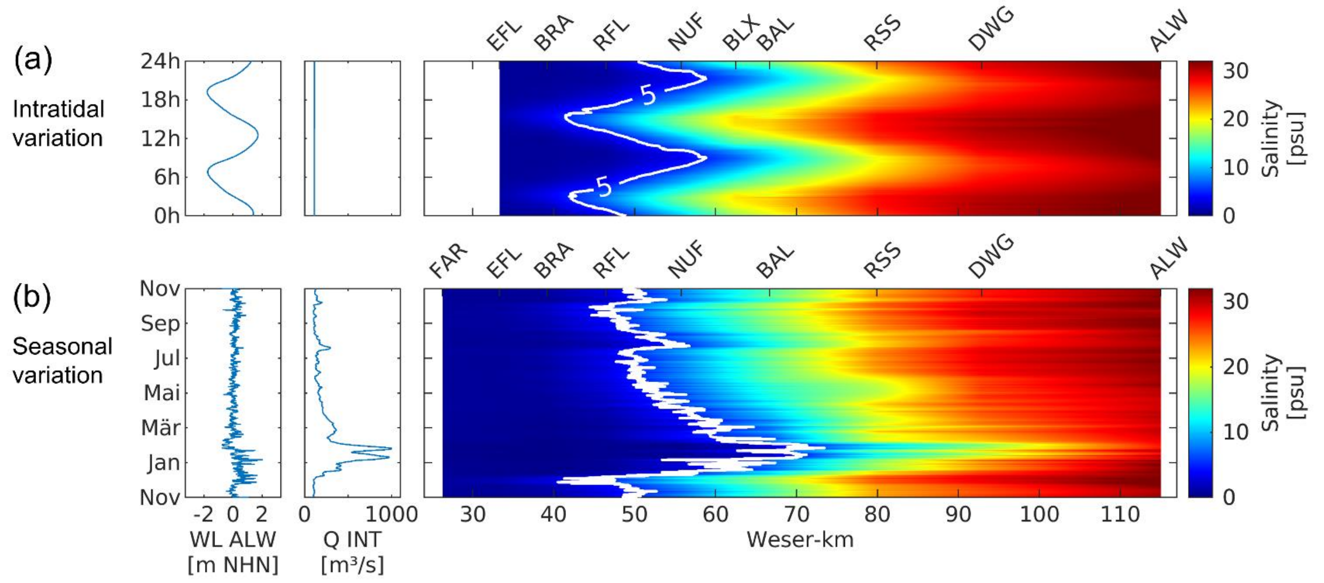

Figure 4. Intratidal and seasonal variation of saltwater intrusion in the Weser estuary. The water level at station Leuchtturm Alte Weser (ALW), discharge at station Intschede (INT), and salinity along the navigation channel of the Weser estuary are displayed on different time scales. Salinity values were interpolated linearly between measurement stations with available measurements along the navigation channel. The 5 psu isohaline is displayed in white. On top, salinity variation within one day, September 1st, 2012, is depicted (a). Below, variation within the hydrological year 2012 of the mean salinity per tidal cycle is depicted (b). We applied a moving median filter to the water level data in (b) to show the seasonal variation (filter size 12h 25min).

4.2 Saltwater intrusion in different system states

Hydrodynamics and saltwater intrusion in the Weser estuary were simulated in hindcast models of 1966, 1972, 1981, and 2012. These models contain respective model topographies and realistic forcing (see Table ~~2~~1) and they were individually calibrated (see ~~Section~~Sect. 3.6). The mean tidal range in the estuary ~~was~~is up to 0.6 m larger in 1981 and 2012 than in 1966

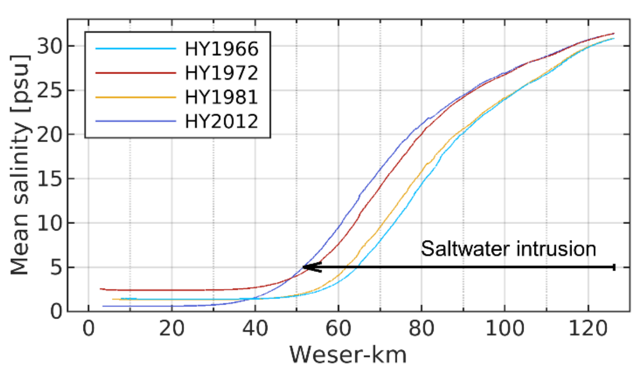

Figure 5 Annual mean, vertically averaged salinity along the navigation channel of the Weser estuary (see Fig. 1) in hindcast models of 1966, 1972, 1981, and 2012.

and 1972 (see Fig. 3a). This reflects the impact of the deepening measures in Lower Weser in 1973–1978, which had a strong effect on tidal dynamics.

Saltwater ~~intruded~~intrudes further in 1972 and 2012 compared to 1966 and 1981 (see ~~).~~Fig. 5). In 1972 and 2012, the 5 psu isohaline ~~was~~is positioned about 10 km more landward. The reason for these large differences is particularly high discharge values in 1966 and 1981, which were on average about twice as high compared to the other system states (see Table ~~5). The~~3). Not all variation can be explained with the discharge conditions~~ fail to explain all variations~~. Compared to 1972, there was higher discharge in 2012; however, the position of the salinity front is about 3 km more landward. In this case, other influencing factors outweigh the impact of discharge. The mean ~~tide~~tidal level at station ALW in system state 2012 ~~is~~was considerably higher compared to 1972, indicating different meteorological conditions and reflecting an increase in mean sea level (Wahl et al., 2013). Moreover, the tidal range at station ALW was larger in 1981 and 2012, possibly due to topography changes (Hubert et al., 2021) and in response to the nodal tide. Along with these factors, changes in topography might affect the differences in the saltwater intrusion.

Table 3. Characteristic conditions in system states 1966, 1972, 1981, and 2012, averaged for one hydrological year based on measured values. Mean salinity and mean discharge were measured at Hemelingen (HEM) and Intschede (INT~~), respectively.~~). Both stations are located upstream of the weir Bremen. Tidal mean water and tidal range in the North Sea were measured at ~~station~~ Leuchtturm Alte Weser (ALW).

Identifier	Mean salinity Weser (HEM)	Mean discharge Weser (INT)	Tidal mean water (ALW)	Tidal range (ALW)
HY1966	1.42 psu	508 $m^3\ s^{-1}$	-0.08 m	2.80
HY1972	2.39 psu	203 $m^3\ s^{-1}$	-0.16 m	2.79
HY1981	1.38 psu	477 $m^3\ s^{-1}$	-0.04 m	2.89
HY2012	0.61 psu	234 $m^3\ s^{-1}$	0.05 m	2.87

4.3 Effect of discharge on saltwater intrusion in different system states

~~The~~The sensitivity of saltwater intrusion to discharge can be described with analytical expressions, which depend on dominant salt flux mechanisms and estuary shape. With a regression analysis (see Sect. 3.5.1), we examined the influence of discharge on the saltwater intrusion length ~~was analysed~~ in ~~each~~all hindcast ~~simulation. The saltwater intrusion length is here defined as the distance from the estuary mouth to the tide-averaged position of the 5 psu isohaline along the navigation channel (see Fig. 1). The estuary mouth is located at Weser-km 126.2.~~simulations. Amongst the simulations, discharge and other parameters differ (realistic forcing, see Table ~~2). Data~~ 1). Two versions of the analysis were ~~processed in the following way to identify correlations between discharge and saltwater intrusion length: First, the saltwater intrusion was calculated for each tidal cycle within the respective hydrological years and discharge conditions were assigned. Data points were then sorted into 50 m³ s⁻¹ bins of discharge between 150–400 m³ s⁻¹ and 100 m³ s⁻¹ bins between 400–1100 m³ s⁻¹ and averaged to reduce the effect of additional influence factors and outliers.~~conducted:~~ If fewer than 10 entries were available for a category, these entries were~~

~~excluded. Based on the resulting average intrusion length for the specified discharge categories, multiple nonlinear regression with interaction effects was performed~~ with and ~~the Levenberg–Marquardt algorithm to obtain trends of the form~~

$$L^* = kQ^m \ , \qquad \text{~~(4)~~}$$

~~with saltwater intrusion length L^*, factor k, discharge Q, and exponent m (see Fig. 6a). The same analysis was performed~~ without pre-processing by data aggregation ~~to examine the method's validity (see Fig. 6b). Plotted with logarithmic axes, m is the gradient of the resulting trend lines.~~ Data from the hindcast simulation of 1972 were excluded ~~from the analysis~~ because the range of discharge values was insufficient for the analysis.

In the scenarios representing 1966, 1981, and 2012, we identified a clear relationship between discharge and saltwater intrusion length according to Eq. (4), with $L \sim Q^{-0.15}$. ~~As expected, the saltwater intrusion length decreases when discharge increases. This effect is greater for low discharge conditions compared to high discharge conditions.~~ In system state 2012, the saltwater intrusion length increases by approximately 9 km if the discharge decreases from 1000 m³ s^{-1} to 380 m³ s^{-1} or from 380 m³ s^{-1} to 150 m³ s^{-1}.

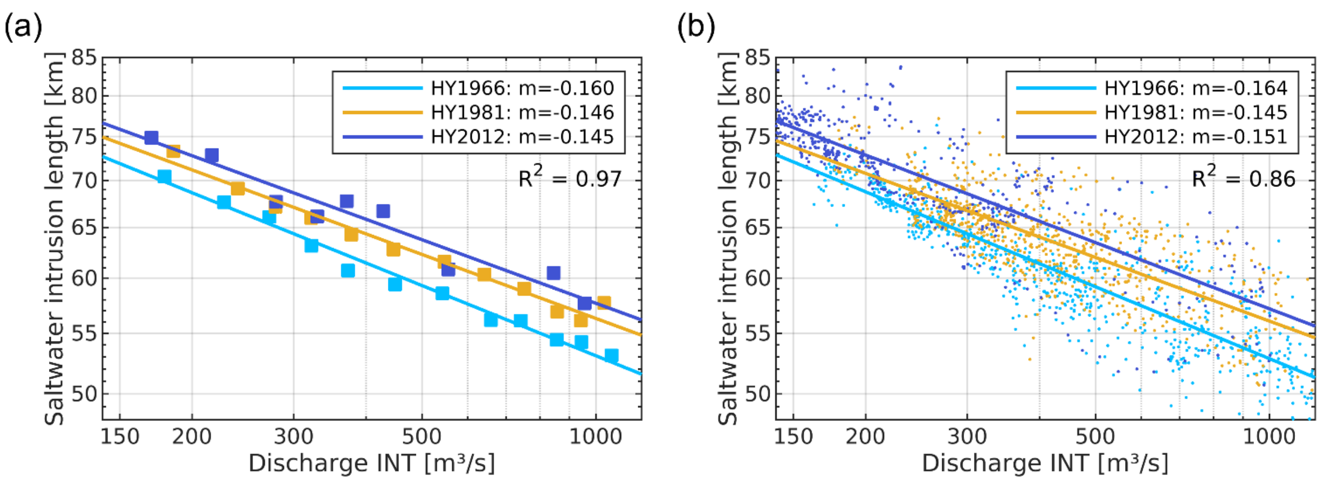

~~**Figure 6. Saltwater intrusion length L* (distance from the estuary mouth at Weser-km 126.2, see Fig. 1, along the navigation channel to tide-averaged 5 psu isohaline) in hindcast models of 1966, 1981, and 2012, in relation to discharge Q measured upstream of weir Bremen at station Intschede (INT). On the left, squares represent the average saltwater intrusion length for different discharge categories and lines represent trends of the form *L*=kQ^m* (a). The analysis was repeated with non-aggregated data points to test the method´s validity (b).**~~

Figure 6. Saltwater intrusion length L* (distance from the estuary mouth at Weser-km 126.2, see Fig. 1, along the navigation channel to the tide-averaged 5 psu isohaline) in hindcast models of 1966, 1981, and 2012, in relation to discharge Q measured upstream of weir Bremen at station Intschede (INT). On the left, squares represent the average saltwater intrusion length for different discharge categories and lines represent trends of the form *L*=kQ^m*. With logarithmic scales, *m* represents the gradient of the lines (a). The analysis was repeated with non-aggregated data points to test the method´s validity (b).

The trend lines for 1966, 1981, and 2012 have comparable gradients in the logarithmic plot (comparable exponents *m*). A significant difference occurs between the exponent in HY1966 compared to the exponent in HY1981 (p~~=~~<0.~~000~~001) and HY2012 (p=0.005) in the regression analysis with non-aggregated datapoints (Fig. 6b).~~6b), pointing to a change in the system between 1966 and 1981. According to Ralston and Geyer , a change in the sensitivity of saltwater intrusion to discharge could indicate a change in salt flux mechanisms. However, it has to be noted that the exact exponents depend on the definition of the saltwater intrusion length. Moreover, not only discharge, but also other influencing factors vary in the examined hindcast simulations.~~

The shift in trend lines indicates that saltwater intrusion increased between 1966 and 1981 and between 1981 and 2012 for similar discharge conditions (see Table 4). For example, with 300 m³ s^{-1} discharge, the saltwater intrusion increased by approximately 2.4 km between 1966 and 1981 and another 1.8 km between 1981 and 2012. This trend could be linked to differences in topography, i.e. the deepening measures conducted in-between the system states.

Table 4. The average landward shift of ~~depth-averaged~~the 5 psu isohaline in the hindcast simulations, based on regression analysis (Fig. 6b).

	1966–1981	1981–2012	Overall shift 1966–2012
150 m³ s^{-1}	1.7 km	2.3 km	4.0 km
300 m³ s^{-1}	2.4 km	1.8 km	4.2 km
1000 m³ s^{-1}	3.2 km	1.1 km	4.3 km

~~The trend lines are differently positioned, which indicates that with similar discharge conditions, saltwater intrusion increased between 1966 and 1981 and between 1981 and 2012. For example, with 300 m³ s-1 discharge, the saltwater intrusion increased by approximately 2.4 km between 1966 and 1981 and another 1.8 km between 1981 and 2012 – however, the exact shift depends on the discharge condition (see Table 6). This trend could be linked to differences in topography, i.e. the deepening measures conducted in-between the system states.~~

4.4 Impact of topography changes on saltwater intrusion

The effect of topography on saltwater intrusion was further examined in simulations with identical boundary values but different model topographies (scenario study). One set of simulations (1966, 1972, 1981, 2012) was conducted with the respective roughness settings, as obtained by calibration of the hindcast models. Another set of simulations was conducted with identical roughness settings (hindcast model 2012).

Simulations with different topographies and respective roughness settings confirm a notable effect of topography changes on saltwater intrusion (see Fig. 7a). The salinity front (5 psu isohaline) shifts landwards between scenario 1972 and 1981 by about 2.5 km, and between 1981 and 2012 by another 1 km. At the same time, the length of the brackish water zone (~~vertically averaged~~ 5 psu isohaline to 20 psu isohaline) increases between the four scenarios from 24.2 km (1966) to 27.6 km (2012~~), as~~

~~the increase in salinity along the river towards the North Sea is more gradual in scenario 2012 compared to the historical system states. The mean intratidal variation slightly decreases between 1966 and 2012.~~).

The differences in saltwater intrusion can be linked to the topography changes between the four system states. The most significant increase in saltwater intrusion occurs between scenarios 1972 and 1981, where considerable deepening measures were conducted in the Lower Weser. An analysis of the mean depth of the navigation channel in the area where saltwater intrusion occurs (Weser-km 40–110) and the position of the ~~vertically averaged~~ 5 PSU isohaline in each of the scenarios suggests a strong link between mean depth and saltwater intrusion (see Fig. 7b). According to that, if the navigation channel is deepened by 1 m in Weser-km 40–110, the position of the 5 psu isohaline shifts landwards by about 2 km.

Deepening measures in the Outer Weser seem to induce an overall extension of the brackish water zone ~~(between 5 psu and 20 psu).~~. Between scenario 1966 and 1972 and between scenario 1981 and 2012, when deepening measures in the Outer Weser were conducted, the length of the brackish water zone increased by 1.1 km and 1.8 km. In contrast, an extension of only 0.5 km occurred between 1972 and 1981 (see Fig. 7a). An extension of the brackish water zone means that salinity increases more gradually towards the sea.

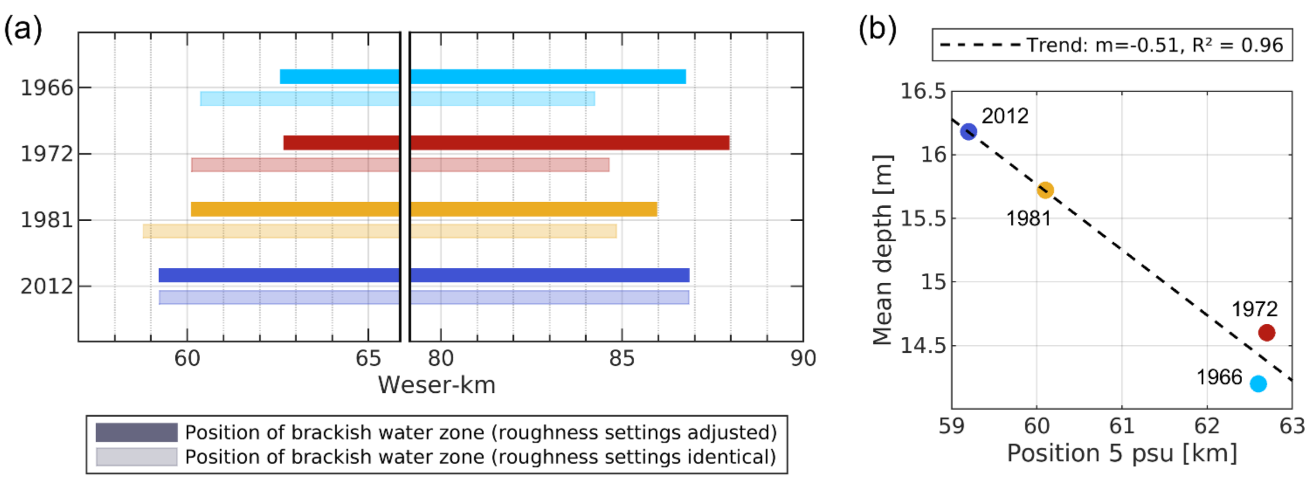

~~**Figure 7. The left diagram (a) shows the effect of topography and roughness variation on the mean position of the brackish water zone (defined as the stretch between the vertically averaged 5 psu and 20 psu isohalines along the navigation channel, see Fig. 1). The dark colours represent simulations of the system states with adjusted roughness settings. The light colours represent simulations with identical roughness settings. On the right (b), the mean position of the vertically averaged 5 psu isohalines in simulations with adjusted roughness settings is displayed in relation to the mean depth of the navigation channel bottom between Weser-km 40 to 100 in simulations of system state 1966, 1972, 1981, and 2012 with identical boundary conditions.**~~

Figure 7. The left diagram (a) shows the effect of topography and roughness variation on the mean position of the brackish water zone (the stretch between the 5 psu and 20 psu isohalines along the navigation channel, see Fig. 1). The dark colours represent simulations with adjusted roughness settings; the light colours represent simulations with identical roughness settings. Forcing is identical. On the right (b), the mean position of the 5 psu isohalines in the simulations with adjusted roughness settings is displayed in relation to the mean depth of the navigation channel between Weser-km 40 to 100.

4.5 Relevance of roughness calibration for the examination of saltwater intrusion in different scenarios

~~Calibration of the roughness settings of the different models considerably improved the model performance (see Table 3). The roughness settings balance out model effects, such as differences in the resolution of original topographic data (see Section 3.2). At the same time, they reflect roughness changes in the physical system due to natural morphological processes and anthropogenic interventions. Thus, the effect of topography cannot be evaluated separately from changes in bottom friction, which occur between the system states.~~

To evaluate the impact of the roughness calibration on the results, we ~~conducted~~compared simulations with different model topographies but with identical roughness settings (settings of hindcast model 2012~~). In addition, we performed~~) to the simulations with individually adjusted roughness settings~~ that were~~, as obtained by calibration of the respective hindcast models. When the roughness settings are identical, ~~the~~ there is no clear trend regarding shifts in saltwater intrusion length ~~is similar in the four scenarios~~between 1966 and 2012. In scenario 1981, salinity values in the Lower Weser are slightly larger than in 2012; in scenario 1966 and 1972, values are slightly lower (see Fig. 7a). ~~Because of the different resolutions of original topographic data, the bathymetry of the historical model topographies is smoother than the model topography of 2012 (see Table 1). In the~~However, simulations with identical roughness settings~~, it can thus be expected that there is less~~ do not adequately reproduce tidal energy~~ dissipation and more landward salt transport~~, e.g. the tidal range in ~~system states 1966, 1972, and~~ 1981 ~~compared~~is larger than in 2012 contrary to ~~2012. This seems to counteract the expected~~ observations. The erroneously increased tidal range exceeds the effect of ~~the topographical differences and approximately balance it out~~changes in other processes, so that the limit of saltwater intrusion ~~barely~~ shifts seawards, and not landwards, between 1981 and 2012.

~~Without awareness of the effects induced by the different resolutions of the original topographic data, the results could lead to the false conclusion that topography has no notable influence on the position of the salinity front. When roughness settings are adjusted according to the calibration results, effects induced by the resolution of the original topographic data are balanced out, tidal dynamics are depicted more correctly, and results suggest that there is an evident influence of topography on the position of the salinity front.~~

4.6 ~~Effect~~Impact of topography changes on ~~processes governing saltwater intrusion~~

~~Saltwater intrusion in estuaries is primarily governed by the~~ tidal effects and estuarine circulation~~, which transports salt landwards, and river flow, which transports it seawards. Channel deepening, straightening, and removal of bedforms change~~

Topography changes can influence tides in the estuary~~ geometry and reduce frictional damping of the tide . This can affect flow volumes and velocities and, specifically, the exchange flow, ~~, e. g. the tidal ~~mixing, and the effectiveness of river discharge. The impact of topographic changes on these~~range may increase due to increasing depths. For the Weser estuary, this effect is confirmed in the simulations with identical forcing. For example, the tidal range at Weser-km 60 increases from 3.65 m in 1966, 3.67 m in 1972, 3.86 m in 1981, to 3.88 m in 2012. This affects saltwater intrusion. Along with tidal effects, other salt transport processes such as the gravitational circulation can change through topography changes. In order to disentangle individual processes ~~was analysed in~~, the scenario simulations of 1966, 1972, 1981, and 2012~~.~~ were analysed. The scenarios contain identical boundary values but different topographies and roughness settings.

4.6.1 Salt flux decomposition

For a better understanding of the salt transport processes, we decomposed the total salt flux through a cross-section in the Lower Weser (Weser-km 60, see Fig. 1) over the period of one spring-neap cycle for each scenario into advective flux, tidal pumping flux, and the estuarine exchange flow (see Sect. 3.5.2). Results of all scenarios (see Fig. 8) indicate that salt is mainly transported into the Weser estuary through tidal pumping. There is also a clear contribution from the estuarine exchange flow, especially in the scenarios 1981 and 2012. Exchange flow and tidal pumping are counteracted by the barotropic flux, which transports salt seawards.

The results indicate that the landward as well as seaward salt transport increased due to the topography changes between 1972, 1981 and 2012. Between 1972 and 1981, the examined cross-section was directly affected by a deepening of the Lower Weser, which seems to induce an increase in estuarine exchange flow by more than threefold. At the same time, a minor increase in tidal pumping occurs and the barotropic flux increases. Between 1981 and 2012, the cross-section is indirectly affected by deepening measures in the Outer Weser. The estuarine exchange flow component slightly decreases and there is an increase in tidal pumping and barotropic flux. Note that the scenarios contain constant river discharge forcing but spring-neap tidal variations. Thus, the position of the brackish water zone varies on the spring-neap cycle but does not show a river discharge driven shift in position. One would expect the total salt flux to be close to zero. However, a seaward total salt flux through the examined cross-section was determined in all scenarios (see Fig. 8), which limits the robustness of our analysis to some extent.

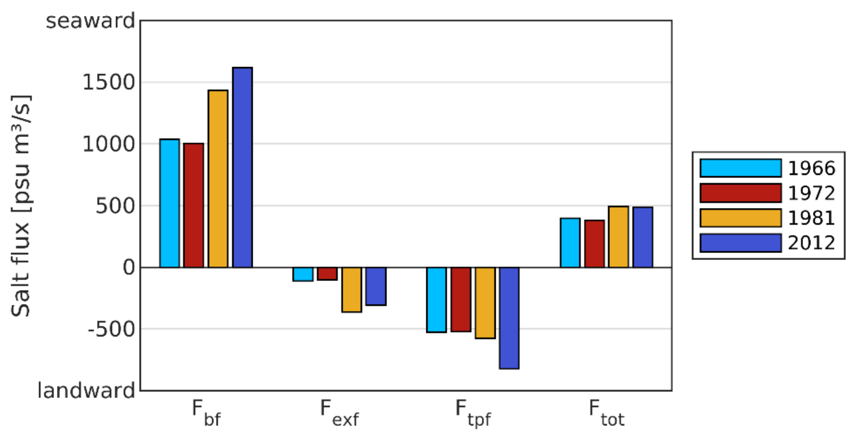

Figure 8. Salt flux through a cross-section in the Lower Weser (Weser-km 60), calculated for the period of one spring-neap cycle based on simulations with identical forcing, but different topography and roughness settings. Displayed are the barotropic flux F_{bf}, the estuarine exchange flow component F_{exf}, the tidal pumping component F_{tpf}, and the total flux F_{tot}.

4.6.2 Exchange flow, according to the Knudsen theorem

~~The~~To verify the method above, we also examined the exchange flow according to the Knudsen theorem (Knudsen, 1900), as described in Burchard et al. (2018b)~~, was applied to quantify exchange flow in the four scenario simulations.~~. Transports through ~~two~~the cross-~~sections~~section in the Lower Weser~~, –~~ (Weser-km ~~55 near Nordenham and Weser-km 65 near Bremerhaven,~~ 60, see Fig 1) were analysed for one spring–neap cycle~~.~~ (same as in Sect. 4.6.1) in the four scenario simulations. Landward and seaward volume transports (Q_{in} and Q_{out}), salt transports ($Q_{in}s_{in}$ and $Q_{out}s_{out}$), and salinity (s_{in} and s_{out}) were determined and time-averaged. ~~Ratios and trends were similar at both cross-sections, but as expected the individual volume transports, salt transports, and salinity values were higher at Weser-km 65.~~

Results indicate that the seaward volume transport is in all scenarios higher than the landward volume transport, reflecting the river discharge input (see Fig. 9). ~~Figure 8 displays results for Weser-km 55.~~ The seaward salt transport is 2 to 4 % higher than the landward salt transport. This corresponds, when adding $Q_{in}s_{in}$ and $Q_{out}s_{out}$, to a residual salt transport (total salt flux) of 388

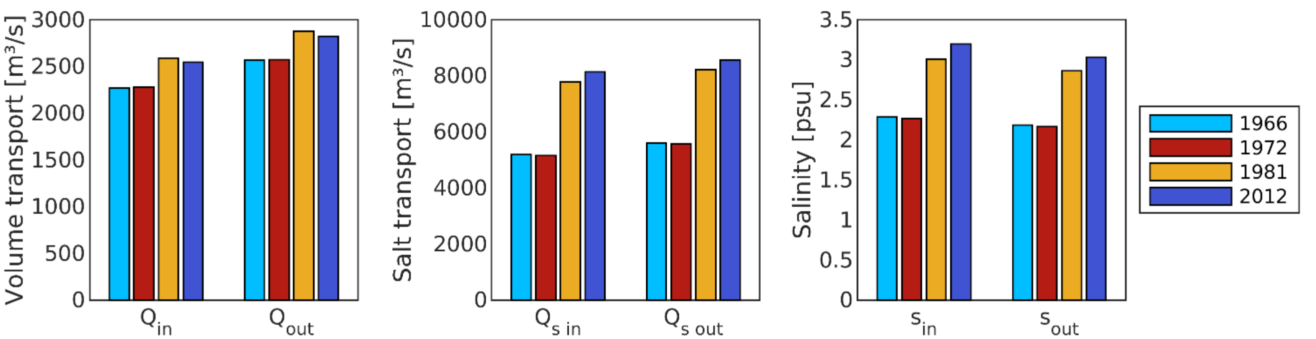

~~**Figure 8. Landward (in) and seaward (out) volume transports (Q), salt transports (Q_s), and salinities (s) through a cross-section in Lower Weser near Nordenham, Weser-km 55, averaged over one spring–neap cycle. In all scenarios, Q_{river} is constant at 300 m^3 s^{-1}.**~~

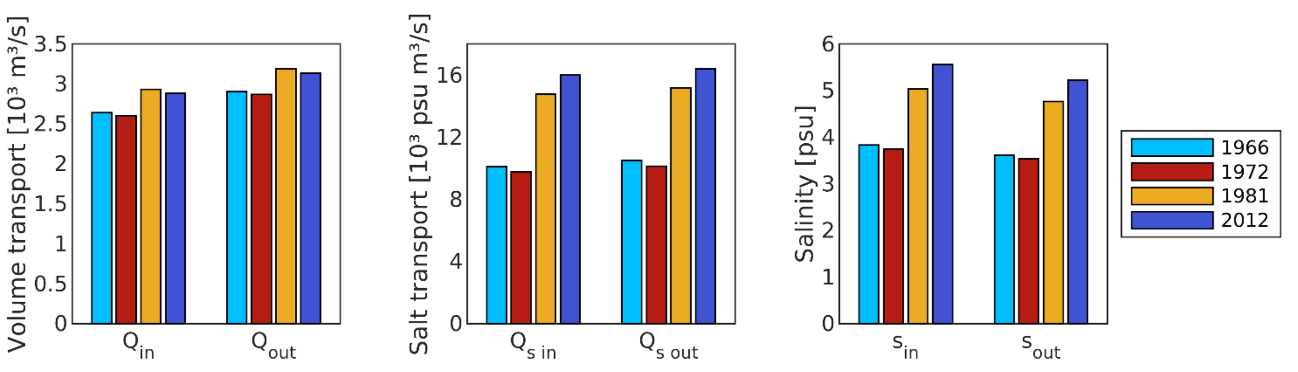

Figure 9. Landward (in) and seaward (out) volume transports (Q), salt transports (Q_s), and salinities (s) through a cross-section in the Lower Weser (Weser-km 60), averaged over one spring–neap cycle. In all scenarios, Q_{river} is constant at 300 m^3 s^{-1}.

(1966), 359 (1972), 418 (1981) and 369 psu m³s^{-1} (2012). This approximately matches the total salt fluxes determined in the salt flux decomposition.

Landward and seaward volume transports increase between 1972 and 1981, probably due to deepening measures in Lower Weser and the associated increase of the tidal volume. ~~As expected, the seaward volume transport is in all scenarios higher than the landward volume transport.~~ However, the ratio of landward to seaward volume transport slightly increases between 1972 and 1981 from 0.~~886~~91 (1966 and 1972) to 0.~~901~~92 (1981 and 2012). ~~Through~~As salt transport in the Lower Weser is primarily governed by tidal processes (see Sect. 4.6.1), this induces an increase ~~of the landward relative to seaward volume transport and river discharge, saltwater intrudes further into the estuary. Thus,~~in salt transport and salinity ~~increase~~ between 1972 and 1981. An additional increase in salt transport and salinity occurs between 1981 and 2012; this cannot be explained by the volume transports.

4.6.~~2 Residual flow and~~ 3 Tidal mixing

As an indicator for tidal mixing

~~As indicators for the estuarine circulation~~, we analysed ~~near-bed and surface residual velocities and~~ the potential energy anomaly (PEA, see Sect. 3.5.3) along the navigation channel of the Weser in the four scenarios and formed an average over one spring–neap cycle. ~~The near-bed residual velocity was extracted 1.5 m above the bed. The residual velocity at the surface and near the bed diverge in approximately the same stretch along the navigation channel where the potential energy anomaly increases, indicating the estuarine gravitational circulation with the seaward residual flow at the surface and landward residual flow at the bottom (see Fig. 9). Compared to 1966 and 1972, landward residual velocities near the bed seem to be slightly stronger in 1981 and 2012 and extend further landwards. These variations indicate a slight increase in the estuarine circulation between these scenarios.~~

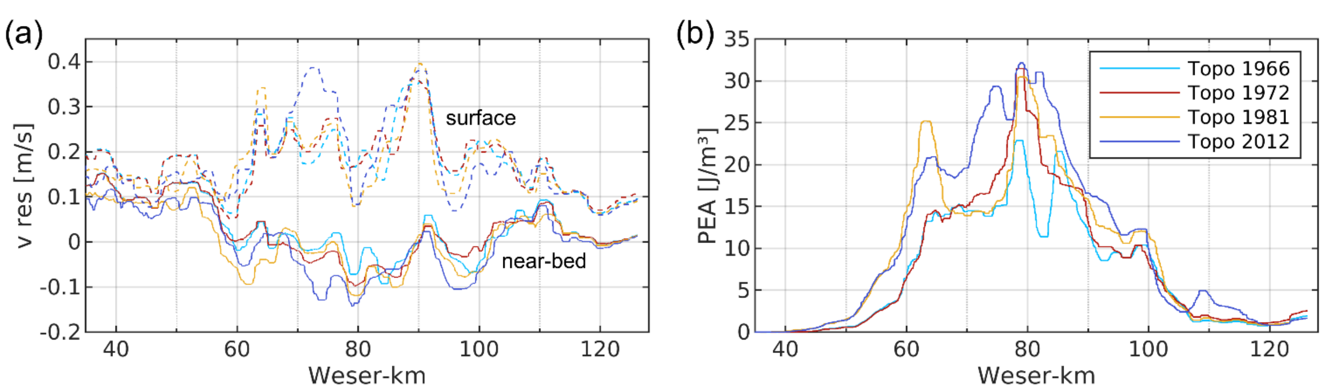

~~**Figure 9. Residual velocity at the surface and near the bed (a) and potential energy anomaly (b) along the navigation channel of the Weser estuary in simulations of different system states with identical boundary conditions, averaged over one spring-neap cycle. We also applied a moving median filter (filter size 2 km) to minimize the importance of local effects.**~~

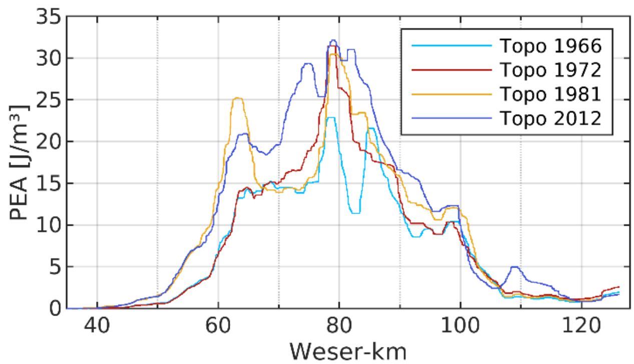

Figure 10. Potential energy anomaly (PEA) along the navigation channel of the Weser estuary in simulations of different system states with identical boundary conditions, averaged over one spring-neap cycle. We applied a moving median filter (filter size 2 km) to minimize the importance of local effects.

In the Weser estuary, stratification is mainly caused by salinity differences within the water column. Thus, the ~~potential energy anomaly (~~PEA~~)~~ is close to zero in the tidal freshwater reach and increases after Weser-km 50 (see Fig. ~~9b~~10). It is largest in Weser-km 70–90, where mean salinity values of 10 psu to 20 psu occur. The spatial distribution and total values of the ~~potential energy anomaly~~PEA differ strongly between the scenarios, indicating differences in the effectiveness of tidal mixing. In Weser-km 50–70, the potential energy anomaly increases more steeply in scenario 1981 and 2012 compared to 1966 and 1972 and reaches higher values than in the other scenarios. Especially high ~~peak~~ values occur in scenario 2012, where the mean potential energy anomaly in Weser-km 70–90 is about 26 J m^{-3}.

~~4.6.3 Effectiveness of river discharge~~

~~In the scenarios study, river discharge was constant and identical. Therefore, the hindcast study simulations examined the effectiveness of river discharge to induce change to the position of the brackish water zone. According to Ralston and Geyer , changes in the sensitivity of saltwater intrusion could indicate a change in salt flux mechanisms. A power-law regression analysis was conducted (see Section 4.2). We could show that no major changes in the sensitivity of saltwater intrusion to discharge occurred. There was a significant change between 1966 and 1981, which was however small. In addition to salinity, other influencing parameters differed between the simulations and lag times in the adjustment of saltwater intrusion to changed conditions were not considered in the analysis. Therefore, the small difference between 1966 and 1981 cannot be clearly attributed to a change in salt flux mechanisms.~~

5. Discussion

Saltwater intrusion is subject to high natural variability and salinity measurements of the past decades are not always available or exhaustive. This makes it difficult to quantify the effect of anthropogenic measures based on measurements only. With numerical simulations, we analysed the impact of anthropogenic measures on saltwater intrusion in two ways: First, we evaluated saltwater intrusion in hindcast-models of the hydrological year 1966, 1972, 1981 and 2012~~. We~~ and analysed ~~the depth-averaged 5 psu isohaline~~it as a function of discharge. Second, we evaluated ~~the~~ saltwater intrusion in a scenario study with identical boundary values~~ (i.e. Q=300 $m^3\ s^{-1}$).~~.

In the model setup, a key challenge was the lower frequency and coverage of historical measurements compared to the present state, i.e. for water level, salinity, and temperature~~.~~ (see Sect. 3.4). This can lead to differences in model accuracy and compromise the comparability of model results. In our case, a detailed validation of the historical models was not possible due to the lack of historical salinity measurements. With a systematic approach and equal treatment of the respective system states, wherever possible, we created consistency and minimized bias. For example, we generated boundary values of all models with identical methods~~, wherever possible,~~ and calibrated each model individually.

~~It was found that~~ In our study, an individual calibration of roughness parameters~~, or at least a careful evaluation of topographical data, is indispensable when setting up models with different topographies. The significance of shifts in roughness with regard to the simulation of different system states has already been highlighted by van Maren et al. . However, models representing historical system states are often not calibrated . We show that, without~~ proved essential (see Sect. 3.6). Without calibration~~ and adjustment of roughness setting for individual model topographies,~~, changes in sediments and bedforms and effects ~~induced by the resolution of the original topographic data can~~of different resolutions of bathymetric data strongly ~~influence~~influenced model results and lead to false conclusions~~. We~~ (i.e. seaward shift instead of landward shift due to topography changes between 1981 and 2012). It has to be noted that calibration is only possible if observational data are available to support a robust calibration. Recalibration with imprecise data of low resolution might even negatively affect model results. In addition, it might not always be necessary, depending on the representation of roughness and sediments, and the resolutions of bathymetric data and grid. However, we recommend that a thorough evaluation of ~~topographical~~bathymetric data and, if needed and possible, calibration of each model should ~~always~~ be conducted when results of models with different topographies are to be compared.~~ An alternative approach to compensate for a low resolution of topographic data is to add artificial surface irregularities, as implemented by Hubert et al. .~~

The analysis of hindcast results showed that, at similar discharge conditions, there is a landward shift in the position of the brackish water zone between 1966–1981 and 1981–2012~~.~~ (see Sect. 4.3). The exact distance of the shift depends on the discharge condition (see Table ~~6~~4). When comparing saltwater intrusion at times with a discharge of 300 $m^3\ s^{-1}$, there is a 2.4 km shift between 1966 and 1981 and a 1.8 km shift between 1981 and 2012. In the scenario study with identical boundary conditions, i.e. Q=300 $m^3\ s^{-1}$, the 5 psu isohaline shifts by 2.5 km between 1972 and 1981 and by 1 km between 1981 and 2012~~.~~ (see Sect. 4.4). Both analyses show that anthropogenic measures in the Weser estuary led to an increase in the saltwater intrusion. This is in agreement with findings for other estuaries, where the navigation channel was also deepened (Andrews et al., 2017; Grasso and Le Hir, 2019; Ralston and Geyer, 2019). In the hindcast study, additional factors such as tides and salinity ~~of the discharge and~~ in the North Sea influence saltwater intrusion. In addition, the evaluation of saltwater intrusion depending on discharge does not account for adaptation time to changing discharge conditions. Nevertheless, results of both the hindcast study and the scenario study indicate an overall shift in the same range, 3.5–4 km. Measures in the Lower Weser, which were conducted in 1973–1978, had the highest impact. However, the exact extent of ~~salt~~saltwater intrusion will also be influenced by factors not included in the model such as changes in tributaries, side channels, and the construction of waterways infrastructure.

The influence of discharge on saltwater intrusion follows the relationship $L \sim Q^{-0.15}$ in our simulations~~.~~ (see Sect. 4.3). Thus, changes in discharge have a higher impact for low discharge ~~conditions~~ than high discharge conditions, in agreement with previous studies (Kösters et al., 2014). Ralston and Geyer (2019) examined the relationship between discharge and saltwater intrusion ~~length~~ in the Hudson river in idealized scenarios with different discharge conditions. For both, bathymetries~~,~~ representing the present state and the predevelopment state, the sensitivity of the saltwater intrusion ~~on~~to discharge follows $L \sim Q^{-0.28}$. The large difference from the sensitivity found in ~~this~~our study ~~(approximately $Q^{-0.15}$) may indicate limitations of the analytical approach, as the funnel-shaped Outer Weser estuary and the heavily engineered channel-like Lower Weser can only be very roughly approximated using analytical descriptions. In addition, different definitions of the saltwater intrusion length and different processes of estuarine mixing~~ could ~~contribute~~be related to ~~the~~ differences in bathymetry and transport processes between the estuaries. ~~Our analysis shows~~While saltwater intrusion into the Hudson is dominated by estuarine exchange flow, we show that the Weser is dominated by tidal pumping (see Sect. 4.6.1). Following Ralston and Geyer (2019), a change in the sensitivity of saltwater intrusion to discharge ~~does not clearly change between the four system states. Following Ralston and Geyer , this indicates that~~could indicate a change in salt flux mechanisms ~~are similar~~. We detect a significant, but very small difference in the sensitivity in 1966 compared to 1981 and 2012 (see Sect. 4.3). However, the exact exponent depends on the definition of the saltwater intrusion length. Moreover, not only discharge, but also other influencing factors vary in the ~~different system states~~examined simulations and lag times in the adjustment of saltwater intrusion to changed conditions were not considered in our analysis. Therefore, the small difference in sensitivity to discharge between 1966 and 1981 cannot be clearly attributed to a change in salt flux mechanisms.

The impact of anthropogenic measures on processes governing saltwater intrusion ~~were~~was further examined based on results of the scenario study (idealized forcing~~). Volume transports~~) (see Sect. 4.6). For all scenarios, a decomposition of the salt flux through a cross-~~sections~~section in the Lower Weser ~~increase~~ was conducted according to Becherer et al. (2016). The salt flux was divided into contributions from advective flux, tidal pumping, and the estuarine exchange flow. Results indicate that salt flux in the Weser estuary is dominated by tidal pumping contributions and advective flux. This also explains the result that saltwater intrusion is further landward during spring tides compared to neap tides (see Sect. 4.1). In contrast, saltwater intrusion in estuaries dominated by estuarine exchange flow decreases during spring tides. Grasso and Le Hir (2019) found that the effect of the spring-neap cycle on saltwater intrusion can change if the governing processes in the estuary change. This aspect could be further examined in subsequent studies. A more thorough study disentangling the role of different processes on seasonal timescales in Weser estuary is presently carried out by Becker (personal communication, July 4, 2022). The estuarine exchange flow through the cross-section strongly increases between 1972 and 1981, ~~indicating~~while tidal pumping increases between 1981 and 2012. In both cases, this is outbalanced by a simultaneous increase of the barotropic flux. A possible interpretation could be that deepening measures in the Weser estuary locally induce an increase in ~~exchange flow. Thereby, landward transport increases more than seaward transport. We also analysed near-bed and surface~~estuarine exchange flow and globally induce an increase in tidal pumping. This aspect could be further explored in future studies, which should also include the analysis at different cross-sections and an analysis of lateral processes. In addition, other decomposition methods could be tested (e.g. Dyer, 1974; Dronkers and van de Kreeke, 1986; Park and James, 1990).

Additionally, the exchange flow through the same cross-section was analysed according to Knudsen (1900), as described in Burchard et al. (2018b). Results confirm a small increase in landward and seaward volume transports (and thus in exchange flow). Representative inflow and outflow salinities are increasing substantially over the years, such that also the salt transports exhibit a strong increase, especially between 1972 and 1981. The residual ~~velocities and~~salt transports determined in the analysis approximately match the total salt fluxes determined in the salt flux decomposition.

An analysis of the potential energy anomaly (PEA) on a transect along the navigation channel of the Weser~~. Results indicate an increase in estuarine circulation and in~~ further indicates that stratification increases between 1972 and 1981 in the Lower Weser due to the deepening of the Lower Weser in 1973–1978. ~~However, fundamental changes in governing processes were not found. Possible limitations of this approach are that~~ It also shows the high variability of tidal mixing along the longitudinal profile, which points the interaction of global trends ~~such as a presumed increase in estuarine circulation are partially overlain with~~and local effects. ~~Local~~In case of the PEA, local effects could comprise e.g. an increased stratification at especially deep stretches ~~or lower residual velocities along the navigation channel in sections where lateral flows prevail. In addition,~~. It has to be noted that the location of the transect is identical in all scenarios and there is deviation from the thalweg on some stretches in case of the historical system states, which could affect the results. ~~Future studies could address these~~These limitations might be overcome by aggregating data over the entire navigation channel rather than analysing data along one transect.

6. Conclusions

Saltwater intrusion in the Weser estuary is highly variable and dependent on natural forcing factors, i.e. river discharge, as well as anthropogenic impacts, i.e. channel deepening. A systematic study of the effect of topography changes on saltwater intrusion was carried out to disentangle these overlapping influencing factors. This study used numerical models of four system states (1966, 1972, 1981, and 2012) with respective topographies to hindcast the historical development of saltwater intrusion (hindcast study) and examine the effect of anthropogenic measures (scenario study). The models were individually calibrated and validated to ~~compensate~~account for ~~different~~ differences in sediments, bedforms, and the resolutions of ~~topographic~~underlying bathymetric data~~, from which the model topographies were generated.~~ .

In the hindcast simulations, the influence of topography is overshadowed by the effect of other factors, particularly discharge. ~~Hydrological years~~ The salinity front is about 10 km more landward in 1972 and 2012 ~~are characterized by low discharge (on average about 220 m^3 s^{-1}), while 1966 and 1981 are high discharge years (about 490 m^3 s^{-1}). Thus, results of the hindcast study show a seaward shift of the mean salinity front in 1966 and 1981 by about 10 km~~ compared ~~with~~to the other ~~two~~ system states~~.~~, as the average discharge is almost double in these years. However, at ~~the same~~similar discharge, a landward shift of the salinity front is indicated between 1966 and 1981 and between 1981 and 2012. This trend is confirmed in the scenario study~~, with~~. With identical boundary values (i.e. Q=~~300m~~300 $m^3 s^{-1}$~~). Between scenario 1972 and 1981,~~), the salinity front shifts landwards by about 2.5 km~~, probably due to deepening measures in the Lower Weser. A landward shift of another 1 km occurs~~ between ~~scenarios~~scenario 1972 and 1981 and by about 1 km between scenario 1981 and 2012. It has to be noted that the exact distance by which the salinity front shifts depends on the discharge due to the nonlinear relation between discharge and saltwater intrusion. Analyses of the salt flux components, the exchange flow, ~~tidal mixing, and sensitivity to discharge~~and stratification indicate that the processes governing saltwater intrusion ~~did not fundamentally change.~~changed only by a small amount in response to anthropogenic measures. However, ~~the~~in the Lower Weser, an increase in estuarine circulation is detected in response to deepening measures in the Lower Weser in 1973~~–~~-1978 ~~caused a small~~and an increase in ~~estuarine circulation and stratification~~tidal pumping in response to deepening in the Outer Weser in 1998–1999.

Author contribution

PK set up the numerical models and conducted simulations and analyses. AZ was involved in conceptualization, design of methodology, and interpretation of the results. PK prepared the initial draft with contributions from AZ. FK, HB and UG contributed to the discussion and revision of the paper. AZ and FK supervised the study.

Competing interests

The authors declare that they have no conflict of interest.

Acknowledgements

The work of PK, AZ and FK was funded by the Federal Waterways and Shipping Administration as part of the project “Änderungen hydrologischer Kenngrößen in der Weser seit 1970 (WeHiKo)”. We thank Ulrike Schiller for her help with regard to historical topographies, Dr. Franziska Lauer for support in generation of artificial neural networks, and Dr.-Ing. Günther Lang for the development of employed postprocessing tools. The work of HB was supported by the project “Processes Impacting on Estuarine Turbidity Zones in tidal estuaries (PIETZ)”, which was funded by the German Research Foundation as BU 1199/24-1. We also thank our two anonymous reviewers who triggered the more complete salt flux analysis and helped to broaden the scope of our study and significantly improve the text.

References

Andrews, S. W., Gross, E. S., and Hutton, P. H.: Modeling salt intrusion in the San Francisco Estuary prior to anthropogenic influence, Continental Shelf Research, 146, 58–81, https://doi.org/10.1016/j.csr.2017.07.010, 2017.

BAW: Historical digital terrain models of the Weser Estuary (HIWEST). Technical Report B3955.02.04.70168-6., Federal Waterways Engineering and Research Institute, https://hdl.handle.net/20.500.11970/107521, 2021.

BAW: Historical digital terrain model data of the Weser Estuary (HIWEST). B3955.02.04.70168-6., Federal Waterways Engineering and Research Institute, https://doi.org/10.48437/02.2020.K2.5200.0001, 2020.

BAW: Mathematical Module Sedimorph: Validation Document Version 1.1, Hamburg, 2002.

Becherer, J., Flöser, G., Umlauf, L., and Burchard, H.: Estuarine circulation versus tidal pumping: Sediment transport in a well-mixed tidal inlet, J. Geophys. Res. Oceans, 121, 6251–6270, https://doi.org/10.1002/2016JC011640, 2016.

Burchard, H., Schulz, E., and Schuttelaars, H. M.: Impact of estuarine convergence on residual circulation in tidally energetic estuaries and inlets, Geophys. Res. Lett., 41, 913–919, https://doi.org/10.1002/2013GL058494, 2014.

Burchard, H. and Hofmeister, R.: A dynamic equation for the potential energy anomaly for analysing mixing and stratification in estuaries and coastal seas, Estuarine, Coastal and Shelf Science, 77, 679–687, https://doi.org/10.1016/j.ecss.2007.10.025, 2008.

Burchard, H., Schuttelaars, H. M., and Ralston, D. K.: Sediment Trapping in Estuaries, Annual review of marine science, 10, 371–395, https://doi.org/10.1146/annurev-marine-010816-060535, 2018a.

Burchard, H., Bolding, K., Feistel, R., Gräwe, U., Klingbeil, K., MacCready, P., Mohrholz, V., Umlauf, L., and van der Lee, E. M.: The Knudsen theorem and the Total Exchange Flow analysis framework applied to the Baltic Sea, Progress in Oceanography, 165, 268–286, https://doi.org/10.1016/j.pocean.2018.04.004, 2018b.

Burchard, H., Hetland, R. D., Schulz, E., and Schuttelaars, H. M.: Drivers of Residual Estuarine Circulation in Tidally Energetic Estuaries: Straight and Irrotational Channels with Parabolic Cross Section, J. Phys. Oceanogr., 41, 548–570, https://doi.org/10.1175/2010JPO4453.1, 2011.

Casulli, V.: A high-resolution wetting and drying algorithm for free-surface hydrodynamics, Int. J. Numer. Meth. Fluids, 60, 391–408, https://doi.org/10.1002/fld.1896, 2008.

Casulli, V. and Walters, R. A.: An unstructured grid, three-dimensional model based on the shallow water equations, International Journal for Numerical Methods in Fluids, 32, 331–348, 2000.

Dijkstra, Y. M., Schuttelaars, H. M., and Burchard, H.: Generation of exchange flows in estuaries by tidal and gravitational eddy viscosity-shear covariance (ESCO), J. Geophys. Res. Oceans, 122, 4217–4237, https://doi.org/10.1002/2016JC012379, 2017.

DIN 4049-1:1992-12: Hydrologie; Grundbegriffe, 2 bis 12.

Dronkers, J. and van de Kreeke, J.: Experimental determination of salt intrusion mechanisms in the Volkerak estuary, Netherlands Journal of Sea Research, 20, 1–19, https://doi.org/10.1016/0077-7579(86)90056-6, 1986.

Dyer, K. R.: The salt balance in stratified estuaries, Estuarine and Coastal Marine Science, 2, 273–281, https://doi.org/10.1016/0302-3524(74)90017-6, 1974.

Geyer, W. R. and MacCready, P.: The Estuarine Circulation, Annual Review of Fluid Mechanics, 46, 175–197, 2014.

Grabemann, I., Krause, G., and Siedler, G.: Langzeitige Änderung des Salzgehaltes in der Unterweser, Deutsche Hydrographische Zeitschrift, 36, 61–77, https://doi.org/10.1007/BF02313285, 1983.

Grasso, F. and Le Hir, P.: Influence of morphological changes on suspended sediment dynamics in a macrotidal estuary: Diachronic analysis in the Seine Estuary (France) from 1960 to 2010, Ocean Dynamics, 69, 83–100, https://doi.org/10.1007/s10236-018-1233-x, 2019.

Hagen, R., Plüß, A., Ihde, R., Freund, J., Dreier, N., Nehlsen, E., Schrage, N., Fröhle, P., and Kösters, F.: An integrated marine data collection for the German Bight – Part 2: Tides, salinity, and waves (1996–2015), Earth Syst. Sci. Data, 13, 2573–2594, https://doi.org/10.5194/essd-13-2573-2021, 2021a.

Hagen, R., Plüß, A., Jänicke, L., Freund, J., Jensen, J., and Kösters, F.: A Combined Modeling and Measurement Approach to Assess the Nodal Tide Modulation in the North Sea, J. Geophys. Res. Oceans, 126, 637, https://doi.org/10.1029/2020JC016364, 2021b.

Hubert, K., Wurpts, A., and Berkenbrink, C.: Interaction of Estuarine Morphology and adjacent Coastal Water Tidal Dynamics (ALADYN-C), Die Küste, 89, 193–217, https://doi.org/10.18171/1.089108, 2021.

Ianniello, J. P.: Tidally Induced Residual Currents in Estuaries of Variable Breadth and Depth, J. Phys. Oceanogr., 9, 962–974, https://doi.org/10.1175/1520-0485(1979)009<0962:TIRCIE>2.0.CO;2, 1979.

Jay, D. A. and Musiak, J. D.: Particle trapping in estuarine tidal flows, J. Geophys. Res., 99, 20445, https://doi.org/10.1029/94JC00971, 1994.

Jay, D. A., Leffler, K., and Degens, S.: Long-Term Evolution of Columbia River Tides, J. Waterway, Port, Coastal, Ocean Eng., 137, 182–191, https://doi.org/10.1061/(ASCE)WW.1943-5460.0000082, 2011.

Knudsen, M.: Ein hydrographischer Lehrsatz, Annalen der Hydrographie und Maritimen Meteorologie, 28, 316–320, 1900.

Kösters, F., Grabemann, I., and Schubert, R.: On SPM Dynamics in the Turbidity Maximum Zone of the Weser Estuary, Die Küste, 81, 393–408, 2014.

Krause, G.: Grundlagen zur Trendermittlung des Salzgehalts in Tide-Ästuarien, Deutsche Hydrographische Zeitschrift, 32, 233–247, https://doi.org/10.1007/BF02226051, 1979.

Lang, G.: Analyse von HN-Modell-Ergebnissen im Tidegebiet, Mitteilungsblatt der Bundesanstalt für Wasserbau, 86, 101–108, 2003.

Lange, D., Müller, H., Piechotta, F., and Schubert, R.: The Weser Estuary, Die Küste, 74, 275–287, 2008.

Liu, W.-C., Ke, M.-H., and Liu, H.-M.: Response of Salt Transport and Residence Time to Geomorphologic Changes in an Estuarine System, Water, 12, 1091, https://doi.org/10.3390/w12041091, 2020.

Malcherek, A.: Gezeiten und Wellen: Die Hydromechanik der Küstengewässer, PRAXIS, Harms, R. and Koch, S. (Eds.), Vieweg +Teubner, 2010.

Milbradt, P., Valerius, J., and Zeiler, M.: Das Funktionale Bodenmodell: Aufbereitung einer konsistenten Datenbasis für die Morphologie und Sedimentologie, Die Küste, 83, 39–63, 2015.

Murphy, A. H.: Skill Scores Based on the Mean Square Error and Their Relationships to the Correlation Coefficient, Monthly Weather Review, 116, 2417–2424, https://doi.org/10.1175/1520-0493(1988)116<2417:SSBOTM>2.0.CO;2, 1988.

NLWKN: Deutsches Gewässerkundliches Jahrbuch: Weser- und Emsgebiet 2015, Hildesheim, 2018.

Park, J. K. and James, A.: Mass flux estimation and mass transport mechanism in estuaries, Limnol. Oceanogr., 35, 1301–1313, https://doi.org/10.4319/lo.1990.35.6.1301, 1990.

Ralston, D. K. and Geyer, W. R.: Response to Channel Deepening of the Salinity Intrusion, Estuarine Circulation, and Stratification in an Urbanized Estuary, J. Geophys. Res. Oceans, 124, 4784–4802, https://doi.org/10.1029/2019JC015006, 2019.

Ralston, D. K., Talke, S., Geyer, W. R., Al-Zubaidi, H. A. M., and Sommerfield, C. K.: Bigger Tides, Less Flooding: Effects of Dredging on Barotropic Dynamics in a Highly Modified Estuary, J. Geophys. Res. Oceans, 124, 196–211, https://doi.org/10.1029/2018JC014313, 2019.

Ralston, D. K., Geyer, W. R., and Lerczak, J. A.: Structure, variability, and salt flux in a strongly forced salt wedge estuary, Journal of Geophysical Research: Earth Surface, 115, 3, https://doi.org/10.1029/2009JC005806, 2010.

Rasquin, C., Seiffert, R., Wachler, B., and Winkel, N.: The significance of coastal bathymetry representation for modelling the tidal response to mean sea level rise in the German Bight, Ocean Sci., 16, 31–44, https://doi.org/10.5194/os-16-31-2020, 2020.

Simpson, J. H.: The shelf-sea fronts: Implications of their existence and behaviour, Phil. Trans. R. Soc. Lond. A, 302, 531–546, https://doi.org/10.1098/rsta.1981.0181, 1981.

Simpson, J. H., Brown, J., Matthews, J., and Allen, G.: Tidal Straining, Density Currents, and Stirring in the Control of Estuarine Stratification, Estuaries, 13, 125, https://doi.org/10.2307/1351581, 1990.

van Maren, D. S., Winterwerp, J. C., and Vroom, J.: Fine sediment transport into the hyper-turbid lower Ems River: The role of channel deepening and sediment-induced drag reduction, Ocean Dynamics, 65, 589–605, https://doi.org/10.1007/s10236-015-0821-2, 2015.

van Rijn, L. C.: Unified View of Sediment Transport by Currents and Waves: I Initiation of Motion, Bed Roughness, and Bed-Load Transport, Journal of Hydraulic Engineering, 133, 649–667, https://doi.org/10.1061/(ASCE)0733-9429(2007)133:6(649), 2007.

Wahl, T., Haigh, I. D., Woodworth, P. L., Albrecht, F., Dillingh, D., Jensen, J., Nicholls, R. J., Weisse, R., and Wöppelmann, G.: Observed mean sea level changes around the North Sea coastline from 1800 to present, Earth-Science Reviews, 124, 51–67, https://doi.org/10.1016/j.earscirev.2013.05.003, 2013.

Wetzel, V.: Der Ausbau des Weserfahrwassers von 1921 bis heute, in: Jahrbuch der Hafenbautechnischen Gesellschaft, edited by: Schwab, R. and Becker, W., Springer Berlin Heidelberg, 1029–1136, 1988.

Wiltshire, K. H., Malzahn, A. M., Wirtz, K., Greve, W., Janisch, S., Mangelsdorf, P., Manly, B. F. J., and Boersma, M.: Resilience of North Sea phytoplankton spring bloom dynamics: An analysis of long-term data at Helgoland Roads, Limnology and Oceanography, 53, 1294–1302, https://doi.org/10.4319/lo.2008.53.4.1294, 2008.

Winterwerp, J. C., Wang, Z. B., Braeckel, A., Holland, G., and Kösters, F.: Man-induced regime shifts in small estuaries - II: a comparison of rivers, Ocean Dynamics, 63, 1293–1306, 2013.